The Grand 4R Four-Bar Based Inherently Balanced Linkage Architecture for synthesis of shaking force balanced and gravity force balanced mechanisms

van der Wijk, Volkert

DOI
10.1016/j.mechmachtheory.2020.103815

Publication date
2020

Document Version
Final published version

Published in
Mechanism and Machine Theory

Mechanism and Machine Theory 150 (2020) 103815

Contents lists available at ScienceDirect

Mechanism and Machine Theory

journal homepage: www.elsevier.com/locate/mechmachtheory

Research paper

The Grand 4R Four-Bar Based Inherently Balanced Linkage Architecture for synthesis of shaking force balanced and gravity force balanced mechanisms

Volkert van der Wijk

Mechatronic System Design, Department of Precision and Microsystems Engineering, Faculty of Mechanical, Maritime, and Materials Engineering, Delft University of Technology, Mekelweg 2, 2628 CD Delft, the Netherlands

ARTICLE INFO

Article history:
Received 6 October 2019
Revised 19 January 2020
Accepted 27 January 2020

Keywords:
Shaking force balance
Gravity balance
Inherent balance
Principal vectors
Four-bar deployable linkage
Center of mass

ABSTRACT

Considering balancing as starting point in the design of mechanisms and manipulators is known as inherent balancing. Inherently balanced linkage architectures then form the basis from which balanced mechanism solutions are synthesized, needing no countermasses contrary to balancing of given mechanisms. In this paper a new and advanced inherently balanced linkage architecture with the 4R four-bar linkage as a basis is presented, the *Grand 4R Four-Bar Based Inherently Balanced Linkage Architecture*. With 24 links it is 26 times overconstrained yet movable with stationary center of mass. It is shown that all theories for tracing the center of mass of a four-bar linkage are found inside. It is shown also how from this architecture a variety of new normally constrained 2-DoF balanced linkages are derived by removing a selection of links. This is done for the situations that all links are mass symmetric, for which 32 solutions are presented, and that all links have a general mass distribution. As an example, the balance conditions for the TWIN-4B, a solution of two similar 4R four-bar linkages, one inside the other, are derived and it is shown how this solution can be transformed into a spatial inherently balanced double Bennett linkage.

1. Introduction

Balanced devices are used in a variety of applications. Shaking force balance together with shaking moment balance, when mechanisms move without resultant reaction forces and reaction moments at the base eliminating base vibrations, is found in high speed robot manipulators [1–4], among others for low settling time [5], dynamic decoupling, and improved stability [6]. It is also known for reducing noise in machinery [7] and for increasing ergonomic comfort in hand tools [8]. Gravity force balance, when gravity does not influence the motion of the mechanism, is applied in robotic manipulators for example to lower actuator torques [9,10], to increase payload capacity [11], and to improve the calibration accuracy [12]. For large deployable structures such as in kinetic architecture gravity force balance is important for stability, safety, and low actuation power [13].

Although shaking force balance is about dynamic (inertial) forces and gravity force balance is about forces within a static force field for which they are two completely different phenomena, they share the same design solutions. Namely, a

E-mail address: v.vanderwijk@tudelft.nl

https://doi.org/10.1016/j.mechmachtheory.2020.103815

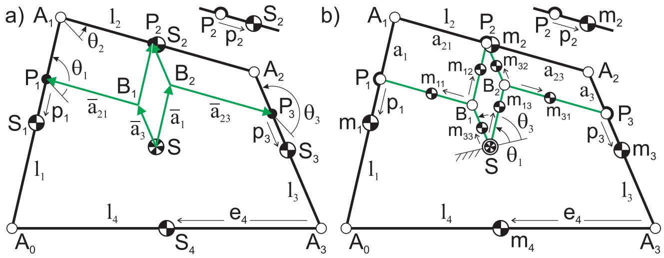

Fig. 1. (a) Principal vectors $\bar{a}_1$, $\bar{a}_{21}$, $\bar{a}_{23}$, and $\bar{a}_3$ describe the motion of the link CoMs with respect to the common CoM in S through principal points P_i; (b) Closed principal vector linkage where the principal vectors have been transformed into rigid links with revolute pairs and mass (both drawn to scale).

shaking force balanced mechanism is gravity force balanced as well. The reverse however is not true, gravity force balanced mechanisms are not shaking force balanced in the direction perpendicular to the gravity force and they are also not shaking force balanced if elements other than (counter-)masses are used such as springs [14]. Since this paper considers balance solutions with solely masses, *force balance* is used to represent both shaking force balance and gravity force balance.

The motivation of this work originated from research on the shaking force balancing of multi-degree-of-freedom (multi-DoF) mechanisms and manipulators. It was observed that common balance methods and approaches for 1-DoF linkages [15,16] lead, because of the required counter-masses and counterrotations, to a significant addition of mass, inertia, and complexity when applied to multi-DoF linkages [17–22] and also to significant elastodynamic problems [23]. The better balance solutions showed some advantageous kinematic or geometric properties. Supported by the idea that the kinematics of multi-DoF manipulators is very flexible - to perform a specific task numerous kinematic solutions of a multi-DoF (parallel) manipulator can be found - this led to the inherent dynamic balance approach where the properties of balance form the basis and are the starting point in the design of balanced mechanisms, which is contrary to the common approach of aiming at finding a balance solution for a given mechanism design [13]. The balance properties are composed in, so-called, inherently balanced linkage architectures: movable compositions of links which solely include the kinematic and geometric relations for balance. From these linkage architectures then, as a next step, design solutions for an intended task can be derived in a variety of ways by possibly altering anything - for example by eliminating, relocating, and resizing links, introducing gears or sliders - and as long as the relations for balance are maintained all results remain inherently balanced.

The method of principal vectors [24] was found fundamental in expressing the properties for balance and for creating the inherently balanced linkages. First open-chain principal vector linkages were developed, showing a strong relation to pantograph linkages and their properties of similarity [25]. Promising results were obtained by synthesis of a 2-DoF dynamically balanced grasper and the DUAL-V high speed 3-DoF dynamically balanced manipulator [3] and also by new designs of large balanced structures such as a movable bridge and a deployable roof structure [13]. Subsequently, various closed-chain principal vector linkages [26] and specific multi-loop linkage architectures based on old graphical methods for tracing the common center of mass (CoM) of linkages were developed [13,27]. Investigating these latter linkage architectures led to the awareness that all of them should be part of a single extensive linkage architecture, a *Grand* Inherently Balanced Linkage Architecture. The preliminary results for the Grand 4R Four-Bar Based Inherently Balanced Linkage Architecture were presented in [28].

The goal of this paper is to present the complete Grand Inherently Balanced Linkage Architecture based on the 4R four-bar linkage and to show in detail how it leads to a variety of inherently balanced mechanism solutions. First the Grand Architecture is shown and explained for mass symmetric links, i.e. links with their CoM on the line through the joints. Subsequently it is shown how a variety of inherently balanced mechanism solutions can be derived from the Grand Architecture and how the known theories for tracing the common CoM of a four-bar linkage are related. Then the Grand Architecture is generalized for mass asymmetric links and it is shown how the inherently balanced mechanism solutions from the generalized architecture differ from the solutions from the Grand Architecture with mass symmetric links. For one inherently balanced mechanism solution, named the TWIN-4B linkage, it is explained how the balance conditions can be derived. At the end an example of a spatial inherently balanced linkage solution is given by transforming the TWIN-4B into a spatial inherently balanced double Bennett linkage. The Appendix presents 32 2-DoF inherently balanced mechanism solutions obtained from the Grand Architecture for mass symmetric links, together with their balance conditions.

2. Composition of the Grand 4R Four-bar Based Inherently Balanced Linkage Architecture

The motions of the CoMs of moving mechanism elements with respect to their common CoM can be described with vectors of constant magnitude known as the *principal vectors* [13,24]. For instance, the motion of the link masses of four elements in a closed chain can be described with respect to their common CoM with the four principal vectors $\bar{a}_1$, $\bar{a}_{21}$, $\bar{a}_{23}$, and $\bar{a}_3$ [13,26]. This is illustrated in Fig. 1a where four links with lengths l_i form a planar linkage with revolute pairs in joints A_0, A_1, A_2, and A_3. Each link here has a mass m_i and is mass symmetric with respect to the line through its joints, which means that the link CoM S_i is located along the line through the joints. The four principal vectors describe a special invariant link point P_i in three of the four links, named the principal points, with which they form three parallelograms.

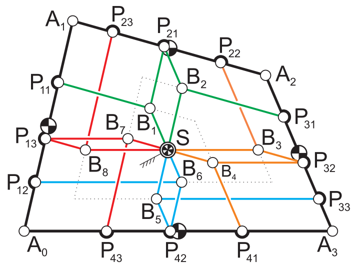

Fig. 2. Linkage architecture based on the combination of the four different principal vector sets. 8 links come together with revolute pairs in S and they can also be merged into the four single links B_1SB_6, B_2SB_5, B_3SB_8, and B_4SB_7.

The principal points can be described with respect to the common CoM of all four links, which is in S, with the principal vectors as:

$$\begin{aligned}\overline{P}_1 &= -a_{21}e^{i\theta_2} + a_3e^{i\theta_3}\\ \overline{P}_2 &= a_1e^{i\theta_1} + a_3e^{i\theta_3}\\ \overline{P}_3 &= a_1e^{i\theta_1} + a_{23}e^{i\theta_2}\end{aligned} \tag{1}$$

with the principal dimensions $a_1 = \|\overline{a}_1\|$, $a_{21} = \|\overline{a}_{21}\|$, $a_{23} = \|\overline{a}_{23}\|$, and $a_3 = \|\overline{a}_3\|$ which are the distances between the points P_1 and A_1, P_2 and A_1, P_2 and A_2, and P_3 and A_2, respectively, and are constants for any motion of the mechanism. The distances between the points P_1 and S_1, P_2 and S_2, and P_3 and S_3 are named p_1, p_2, and p_3, respectively. These equations are linear combinations of the time dependent unit vector of each rotational DoF θ_i. They hold for both the situation that link 4 is eliminated and the resulting open chain has three DoFs as well as for the depicted closed chain with two DoFs where θ_1, θ_2, and θ_3 have dependency.

Because of their constant lengths, the principal vectors can be transformed into real rigid links as shown in Fig. 1b. These principal vector links have lengths a_1, a_{21}, a_{23}, and a_3 and have revolute pairs in P_1, P_2, P_3, B_1, B_2, and S. S here is the common CoM of all 10 links and is an invariant link point in both links B_1S and B_2S. The complete linkage is force balanced about S and when S is kept as a fixed point in the base then a force balanced linkage with two DoFs is obtained.

The linkage in Fig. 1b is referred to as a closed-chain principal vector linkage of which all the links are mass symmetric. The masses of the principal vector links m_{11}, m_{12}, m_{13}, m_{31}, m_{32}, and m_{33}, have their CoM along the line through their joints at a distance p_{11}, p_{12}, p_{13}, p_{31}, p_{32}, and p_{33}, respectively, from the joints as indicated by the arrows. The balance conditions for which the common CoM is in joint S for all motions can be derived from the conditions of the general version where the links have a generally located link CoM [13,26] as:

$$\begin{aligned}m_1p_1 &= (m_2 + m_3 + m_4 + m_{31} + m_{32})a_1 - m_4\frac{e_4}{l_4}l_1 + m_{12}p_{12} + m_{13}p_{13}\\ m_2p_2 &= \left(m_1 + m_4\frac{e_4}{l_4}\right)a_{21} - \left(m_3 + m_4\left(1 - \frac{e_4}{l_4}\right)\right)a_{23} + m_{11}p_{11} - m_{31}p_{31}\\ m_3p_3 &= (m_1 + m_2 + m_4 + m_{11} + m_{12})a_3 - m_4\left(1 - \frac{e_4}{l_4}\right)l_3 + m_{32}p_{32} + m_{33}p_{33}\end{aligned} \tag{2}$$

where a_{21} and a_{23} are related by l_2 as $a_{21} + a_{23} = l_2$. In the Appendix the linkage of Fig. 1b is shown as linkage solution 1 with an alternative notation of these balance conditions. To give a realistic image, Fig. 1 was drawn to scale for m_1, m_2, m_3, and m_4 located halfway their links with values proportional to their link lengths ($\frac{m_1}{l_1} = \frac{m_2}{l_2} = \frac{m_3}{l_3} = \frac{m_4}{l_4}$) with the other masses equal to zero. If the mass of the other links is included then S shifts a little closer to link 2 for which the parallelograms become slightly smaller.

In Fig. 1b only one of the four possible ways to construct principal vector links in a closed chain of four links is shown, which can be seen as that the parallelograms are centered about link 2. It is also possible to construct the parallelograms about link 1, link 3, or link 4 of which the results look similar. When all four of them are combined into the same linkage, then the result in Fig. 2 is obtained where eight links connect with revolute pairs in S. This linkage architecture is based on the four different principal vector sets and has three principal points in each of the four-bar links. For clarity of the illustration the masses of the principal vector links were not drawn.

With the eight links connecting in S the linkage architecture is 6 times overconstrained yet movable. Since each opposite pair of links moves as if it is a single rigid link, the eight links can be transformed into the four single links B_1SB_6, B_2SB_5, B_3SB_8, and B_4SB_7 with S as their common joint. In that case the linkage architecture is 10 times overconstrained yet movable.

In the architecture of Fig. 2 links $P_{31}B_2$ and $P_{43}B_7$ can be extended to a common joint C_1. Also links $P_{11}B_1$ and $P_{41}B_4$ can be extended to a common joint C_2, links $P_{22}B_3$ and $P_{12}B_6$ can be extended to a common joint in C_3 and links $P_{33}B_5$ and $P_{23}B_8$ can be extended to a common joint in C_4. In Fig. 3 these extensions are included with revolute pairs in joints C_i. Revolute pairs in joints D_1, D_2, D_3 and D_4 are also included, which is possible since the links intersect at invariant link points for all motions, forming parallelograms.

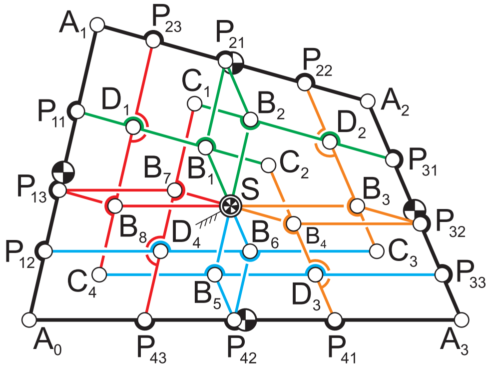

Fig. 3. The *Grand 4R Four-Bar Based Inherently Balanced Linkage Architecture* including the extended links with joints C_i and the joints D_i. The common CoM of all 24 links in S for all motions.

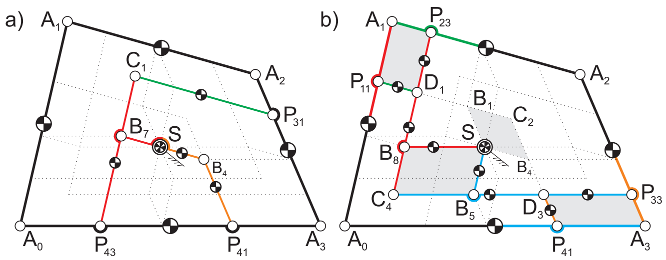

Fig. 4. (a) Inherently balanced linkage with S as a coupler point of a similar four-bar linkage, connected through double contour linkage $P_{43}C_1P_{31}$; (b) Inherently balanced linkage with three pantographs, shown with the two possible pantographs in the center which form a Burmester's focal mechanism.

The resulting architecture in Fig. 3 will be referred to as the *Grand 4R Four-bar Based Inherently Balanced Linkage Architecture*. It shows the complete composition of the kinematic conditions for inherent balance with a 4R four-bar linkage as a basis. With the four links passing through S the architecture is 26 times overconstrained yet movable. Also here S is the common CoM of all 24 links for any motion. In the next section it is shown that because of the high number of overconstraints a wide variety of normally constrained inherently balanced mechanism solutions can be derived from this Grand Architecture.

3. Synthesis of normally constrained inherently balanced linkage solutions

The Grand Architecture in Fig. 3 can be used as the starting point in the design of a balanced mechanism or manipulator for an intended task. Every mechanism that is derived from the Grand Architecture without violating the kinematic geometry has inherent balance properties. This means that then with a specific combination of mass parameter values, calculated from the balance conditions, the resulting mechanism is balanced with respect to joint S, the base pivot, without the need of additional masses or elements. With this approach balancing is considered before the (final) design of the mechanism of which the topology then depends primarily on advantageous balance capability instead of other reasons for the choice of the initial mechanism topology.

First it is shown how normally constrained 2-DoF linkage solutions can be derived from the Grand Architecture which relate to known theory on the motion of the common CoM, followed by examples of other 2-DoF linkage solutions. When from the Grand Architecture in Fig. 3 all internal links are removed but links $P_{31}C_1$, C_1P_{43}, B_7B_4, and B_4P_{41}, then the normally constrained linkage in Fig. 4a is obtained where S, an invariant point in link B_7B_4, is the common CoM of all 8 links. In this solution a four-bar $P_{43}B_7B_4P_{41}$ can be observed that is similar to and smaller than the fourbar $A_0A_1A_2A_3$, sharing link A_3A_0. This is related to the theory of Kreutzinger [29] who found that the common CoM of the three moving links of a four-bar linkage traces a coupler curve of a similar four-bar linkage which is also similar to a coupler curve of the linkage itself. Where Kreutzinger used this similar fourbar linkage as a graphical tool for analysis, here the similar fourbar is a real linkage of which the masses are included as well.

The extension of link $P_{43}B_7$ to C_1 and link C_1P_{31} together constrain the four-bar linkage $P_{43}B_7B_4P_{41}$ to move synchronously with four-bar linkage $A_0A_1A_2A_3$. In fact, links $P_{43}C_1$ and C_1P_{31} form together with links A_0A_3 and A_2A_3 another similar four-bar linkage. This is related to the theory of Shchepetil'nikov [30] who named it a *double contour transformation* where links $P_{43}C_1$ and C_1P_{31} are the double contour of links A_0A_1 and A_1A_2 and subsequently links $P_{41}B_4$ and B_4B_7 are the double contour of links A_3P_{31} and $P_{31}C_1$. With this method the graphical analysis of the motion of the common CoM could be more accurate

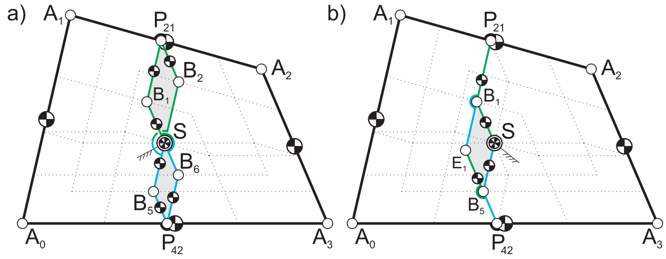

Fig. 5. (a) Inherently balanced linkage with a single pantograph to two opposite four-bar links; (b) Inherently balanced linkage with design variation of the pantograph in Fig. 5a.

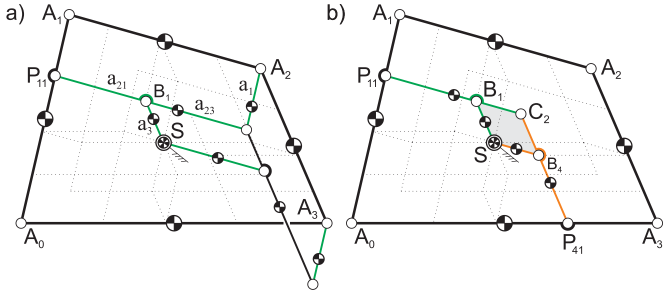

Fig. 6. (a) Design variation of the inherently balanced linkage in Fig. 1b; (b) Inherently balanced linkage solution with a single pantograph to two connecting four-bar links.

and less cumbersome as compared to the method of principal vectors, which was also invented for graphical analysis of the motion of the common CoM of a system of rigid bodies [31].

Within the Grand Architecture in Fig. 3 numerous similar four-bar linkages can be found. Of the solution in Fig. 4a 8 versions can be found which are essentially equal, two with respect to each link of the four-bar $A_0A_1A_2A_3$, a left and a right one. For instance the version with links $P_{11}B_1$, B_1B_6, $P_{12}C_3$, and C_3P_{22} is left oriented and with respect to four-bar link A_0A_1.

When within the Grand Architecture all links are removed but links $P_{11}D_1$, $P_{23}D_1$, D_1C_4, C_4D_3, B_8S, B_5S, $P_{33}D_3$, and $P_{41}D_3$, then the solution in Fig. 4b is obtained. This solution can be regarded as a combination of three balanced pantographs where pantograph $A_0A_1A_2P_{11}D_1P_{23}$ traces the common CoM of its four links in D_1. Similarly the pantograph $A_2A_3A_0P_{33}D_3P_{41}$ traces the common CoM of its four links in D_3. The third pantograph $D_1C_4D_3B_5SB_8$ connects to the mass centers of the two other pantographs and traces the common CoM of all three pantographs in S. This solution is related to the graphical method of Fisher to determine the common CoM of all body segments of a human in motion [24].

It is noted that in Fig. 4b links $P_{23}D_1$ and D_1C_4 are two separate links and also $P_{33}D_3$ and D_3C_4 are two separate links. Since the size of a pantograph does not affect its properties of similarity or scaling, the link lengths of the central pantograph can be chosen freely such that link D_1C_4 is no longer in line with link $P_{23}D_1$ and link D_3C_4 is no longer in line with link $P_{33}D_3$. This holds also for the two other pantographs that therefore need not to be embedded within the links of the four-bar linkage.

For the solution in Fig. 4b there exist 4 versions within the Grand Architecture. For the central pantograph also links D_1C_2, C_2D_3, B_1S, and SB_4 could be chosen for which along the diagonal A_1A_3 two pantograph versions are found. Similarly two versions of three pantographs can be found along the diagonal A_0A_2. It is interesting to note that the two central pantographs together form a well known Burmester's focal linkage with S as the focal point [32,33]. This means that within the Grand Architecture two Burmester's focal linkages are found.

By removing all internal links from the Grand Architecture but the links $P_{21}B_1$, B_1B_6, B_6P_{42}, $P_{42}B_5$, B_5B_2, and B_2P_{21} the inherently balanced solution in Fig. 5a is obtained. These links form a single pantograph with the common CoM of all 10 links in S, the joint between links B_1B_6 and B_5B_2. This solution is related to the theory of Dobrovol'skii [34] where a single pantograph connected to the two opposite four-bar links is used as a graphical tool for analysis of the motion of the common CoM of the four-bar linkage. From Fig. 5a it is found that the connection points of the pantograph with the four-bar linkage are principal points, an interesting new finding.

Dobrovol'skii presented the pantograph in the form shown in Fig. 5b, which is a design variation of the pantograph in Fig. 5a where E_1 is a joint between the extended links $P_{21}B_1$ and $P_{42}B_5$ and joints B_2 and B_6 are removed. As explained for the pantographs in Fig. 4b, also this pantograph may have any shape for the same property of similarity or scaling, keeping the ratio $P_{21}S$: $P_{42}S$ constant.

Fig. 6a shows a variation of the principal vector linkage in Fig. 1b, also an inherently balanced linkage solution. This solution is related to the theory of Artobolevskii [35] in which the principal vectors are used as a graphical tool in a slightly different way with the active use of only one principal point, P_{11}.

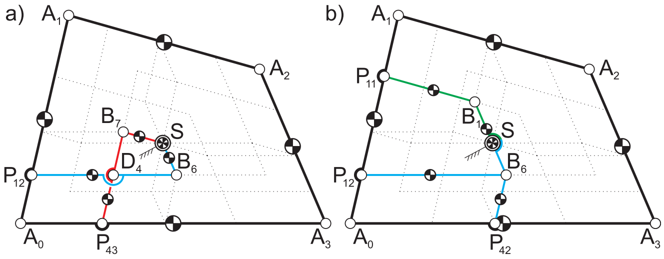

Fig. 7. Inherently balanced linkage (a) with centered similar four-bar connected by a parallelogram; (b) with similar four-bar and a connecting link to a side.

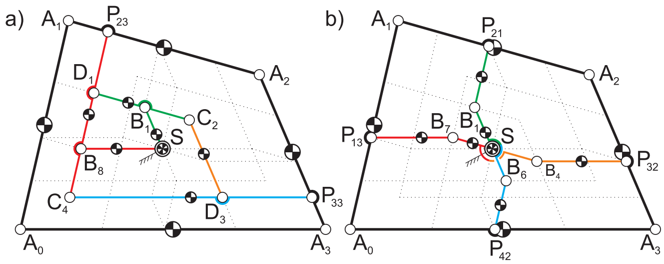

Fig. 8. Inherently balanced linkage (a) with centered similar four-bars; (b) without any similar four-bar or parallelogram.

Herewith the inherently balanced linkage solutions derived from the Grand Architecture that are related to a known theory have been found. However there still are numerous other inherently balanced linkage solutions that can be derived. For instance by removing all internal links from the Grand Architecture but links $P_{11}C_2$, C_2P_{41}, B_1S, and SB_4 the solution in Fig. 6b is obtained. This solution shows that the common CoM of all 8 links is in S for all motions, which is a joint of a single pantograph connected in principal points P_{11} and P_{41} with the four-bar linkage. This means that in addition to the solution in Fig. 5b, a single pantograph can also be connected to two connecting four-bar links for inherent balance.

In Fig. 7a an inherently balanced solution is shown that is obtained when from the Grand Architecture all internal links are removed but links $P_{12}B_6$, B_6S, SB_7, and B_7P_{43}. The result is a small similar four-bar linkage that is connected to the outer four-bar linkage by means of a parallelogram. Fig. 7b shows the inherently balanced solution obtained by removing from the Grand Architecture all internal links but links $P_{11}B_1$, B_1B_6, B_6P_{12}, and B_6P_{42}. The result is a similar four-bar linkage as in Fig. 4a, however here it is constrained with the outer four-bar through link B_6P_{42}, forming a parallelogram.

Fig. 8a shows the result of an inherently balanced linkage obtained by solely keeping links $P_{23}C_4$, C_4P_{33}, D_1C_2, C_2D_3, B_1S, and SB_8 inside the Grand Architecture. This is a different combination of similar four-bar linkages which is more centered as compared to the solution in Fig. 4a. The result in Fig. 8b is obtained by removing all internal links from the Grand Architecture but links $P_{21}B_1$, B_1B_6, B_6P_{42}, $P_{13}B_7$, B_7B_4, and B_4P_{32}. The common CoM of all 10 links is in S, which is the joint between links B_1B_6 and B_7B_4. With respect to the results so far, this inherently balanced linkage has no parallelograms neither similar four-bar linkages.

In total 32 different inherently balanced linkage solutions have been derived from the Grand Architecture in Fig. 3, which are presented in the Appendix together with their balance conditions.

4. Generalization for mass asymmetric links

When the link CoM is not located along the line through the joints of the link but at a certain offset from this line, then the link is mass asymmetric. This is the general case while mass symmetric links can be seen as a specific case, however simpler and more common in real applications. Fig. 9 presents the Grand 4R Four-Bar Inherently Balanced Linkage Architecture where all links are mass asymmetric and S is the common CoM for all motions. As compared to the mass-symmetric case in Fig. 3, here the principal points do not lay along the line through the joints and various internal links have become triangular elements, such as link $P_{12}B_6C_3$ where B_6 is not on the line through P_{12} and C_3. Segment $P_{12}B_6$ is parallel to line A_0P_{42} and segment B_6C_3 is parallel to link B_4P_{32} and to line $P_{41}A_3$. Another difference is that joints D_i do not exist for the general case. This has as a direct consequence that the general architecture is only 18 times overconstrained and that the number of normally constrained inherently balanced linkage solutions that can be derived from the general architecture is significantly lower.

The General Grand Architecture was drawn to scale with the parameter values in Table 1 as explained in Fig. 10 which is without including the mass of the internal links. The composition of the general architecture is analogous to the mass symmetric architecture by combining four general closed-chain principal vector linkages which were obtained and precisely

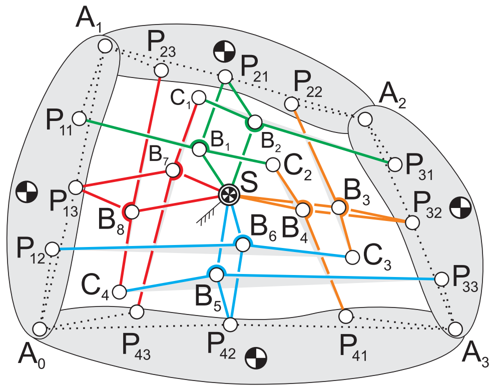

Fig. 9. Grand 4R Four-bar Based Inherently Balanced Architecture for general mass distributions of the links.

Table 1
Parameter values of the General Grand Architecture drawn in Fig. 9 and Fig. 10.

(cm)	(kg)	(cm)	(cm)
$l_1 = 70$	$m_1 = 8.0$	$e_1 = 0.55 \cdot l_1$	$f_1 = 0.15 \cdot l_1$
$l_2 = 65$	$m_2 = 6.7$	$e_2 = 0.43 \cdot l_2$	$f_2 = 0.10 \cdot l_2$
$l_3 = 55$	$m_3 = 6.5$	$e_3 = 0.52 \cdot l_3$	$f_3 = 0.23 \cdot l_3$
$l_4 = 100$	$m_4 = 5.5$	$e_4 = 0.48 \cdot l_4$	$f_4 = 0.07 \cdot l_4$

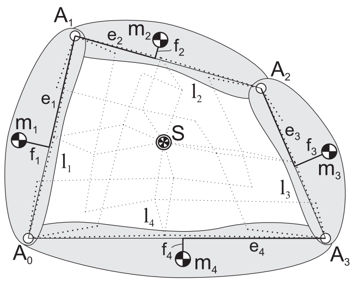

Fig. 10. Illustration of the link CoM parameters for the architecture in Fig. 9 (drawn to scale).

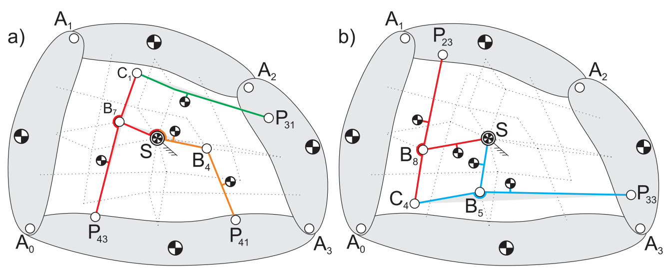

Fig. 11. Inherently balanced linkage solutions with mass asymmetric links (a) generalized from Fig. 4a; (b) generalized from Fig. 6b.

calculated in [13,26]. Also here there are eight links coming together in joint S, which also can be merged into the four ternary elements B_1SB_6, B_2SB_5, B_3SB_8, and B_4SB_7 with S as common joint.

The inherently balanced linkage solutions that can be derived from the General Grand Architecture are comparable of topology with the solutions obtained from the mass symmetric case. For instance Fig. 11a shows the solution of Fig. 4a for links with a generally located CoM. All three links $P_{43}B_7C_1$, $P_{31}C_1$, and B_7SB_4 have an angle instead of being straight links as in Fig. 4a.

In Fig. 11b the solution for general mass distributions of the linkage in Fig. 6b is shown. Also here links $P_{23}B_8C_4$ and $P_{33}B_5C_4$ have an angle at B_8 and B_5, respectively. Fig. 12a shows an inherently balanced solution comparable to Fig. 8b where links B_1SB_6 and B_3SB_8 have an angle at their common joint in S. In Fig. 12b an inherently balanced linkage solution

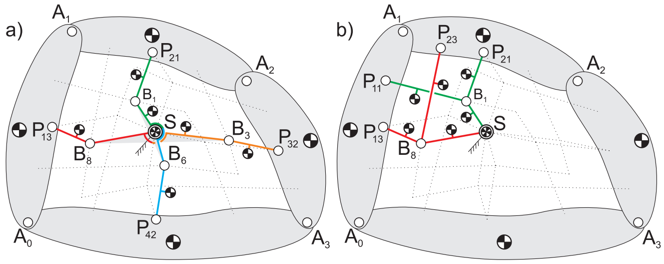

Fig. 12. Inherently balanced linkage solutions with mass asymmetric links (a) generalized from Fig. 8b; (b) closely related to Fig. 7a with two additional links.

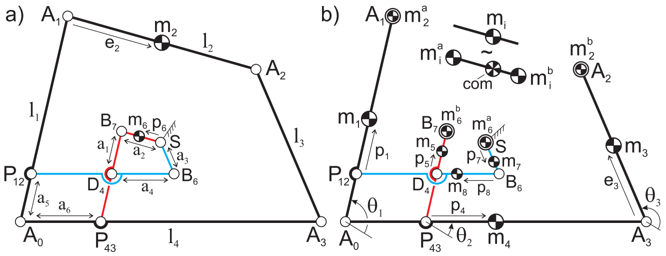

Fig. 13. (a) TWIN-4B inherently balanced linkage with link parameters; (b) 3-DoF open loop model with mass parameters and equivalent masses substituting links 2 and 6.

is shown that is closest to the solution in Fig. 7a. Since for general mass distributions joints D_i do not exist, two additional links $P_{13}B_8$ and $P_{21}B_1$ are required to constrain the motion normally. In this solution all links are straight.

5. Deriving the balance conditions: example of the TWIN-4B

After the choice of an inherently balanced linkage solution as starting point in the design, the next step is to obtain the relations among the mass parameter values for which the linkage is balanced. These relations are known as the balance conditions. In this section it is shown, as an example, how the balance conditions are derived for the linkage in Fig. 7a, which will be referred to as TWIN-4B linkage.

In Fig. 13 the TWIN-4B linkage is shown with its design parameters. The balance conditions in fact consist of two groups of conditions. The first group of balance conditions are the kinematic balance conditions and follow from the properties of similarity as determined by the Grand Architecture and can be written from Fig. 13a as:

$$\frac{a_1}{l_1} = \frac{a_2}{l_2} = \frac{a_3}{l_3} = \frac{a_4}{l_4} \tag{3}$$

for similarity of the two four-bars and $|\overline{A_0P_{12}}| = |\overline{P_{43}D_4}| = a_5$ and $|\overline{P_{12}D_4}| = |\overline{A_0P_{43}}| = a_6$ defining the parallelogram $A_0P_{12}D_4P_{43}$. Since these properties of similarity are completely defined by the design of the links, they turn out to be purely geometric conditions. The second group of balance conditions are the mass balance conditions which determine the relations among the link mass values and their centered location in each link. These conditions can be derived with a method where the linkage obtains three relative degrees of freedom and writing the linear momentum equations of each relative DoF individually [13,26]. This takes advantage of the characteristic that the linear momentum of a force balanced mechanism is constant (zero) for any of its motions.

The first step is to model the linkage as an open loop linkage with three degrees of freedom. This can be done in multiple ways such as the one illustrated in Fig. 13b where link 2 (A_1A_2) and its parallel link 6 (B_7S) are eliminated and substituted with equivalent masses. The mass m_2 of link 2 is modeled with equivalent masses m_2^a and m_2^b located in A_1 and A_2, respectively, where mass equivalence is determined by $m_2^a + m_2^b = m_2$ and $m_2^a e_2 = m_2^b(l_2 - e_2)$. The mass m_6 of link 6 is modeled similarly with equivalent masses m_6^a and m_6^b located in S and B_7, respectively, where mass equivalence is determined by $m_6^a + m_6^b = m_6$ and $m_6^a p_6 = m_6^b(a_2 - p_6)$. Another option which is similar is to substitute link 3 (A_2A_3) and its parallel link 7 (SB_6). These are the two simple options, since substituting either link 1 (A_0A_1) or link 4 (A_3A_0) with their parallel link would disconnect the inner links from the outer links. In that case the geometry of the grand architecture is needed as graphical tool for analyzing the individual motions of each relative DoF, which is more complicated. As shown in Fig. 13b, parallelograms not related to the substituted links do not need to be opened.

The second step then is to write the linear momentum equations for the individual motion of each of the three DoFs and equal them to the linear momentum of the total mass moving in S, the desired common CoM. The individual motion means rotation of one of the three principal elements (here links 1, 3, and 4) about any point with its parallel links rotating

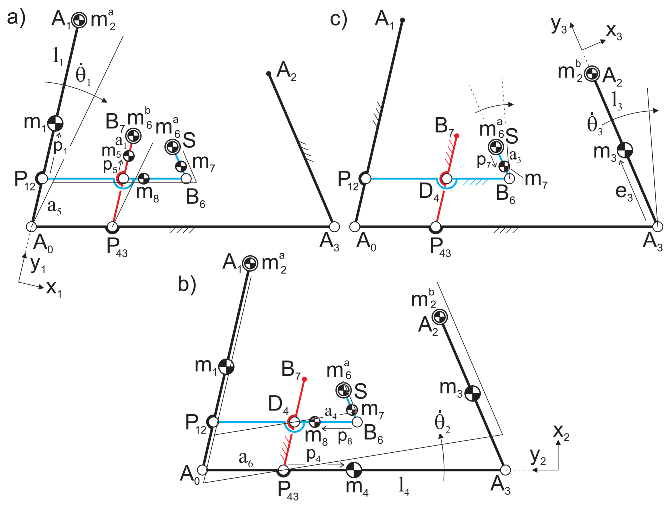

Fig. 14. (a) Motion of the first relative DoF; (b) Motion of the second relative DoF; (c) Motion of the third relative DoF. With the linear momentum equations of these motions the mass balance conditions are obtained readily.

synchronously while all other links solely translate or are immobile [13,26]. In Fig. 14a one possibility of the motion of the first DoF is illustrated where link 1 rotates about A_0, link 5 rotates about P_{43}, links 3 and 4 are immobile and links 7 and 8 have solely translational motion. The linear momentum L_1 of this motion can be written with respect to reference frame x_1y_1, which is aligned with A_0A_1 as illustrated, and must be equal to the linear momentum of the total mass moving in S:

$$\frac{L_1}{\dot{\theta}_1} = \begin{bmatrix} m_1(a_5+p_1) + m_2^a l_1 + m_5(a_5+p_5) + \\ m_6^b(a_5+a_1) + (m_6^a + m_7 + m_8)a_5 \\ 0 \end{bmatrix} = \begin{bmatrix} m_{tot}a_5 \\ 0 \end{bmatrix} \tag{4}$$

with the total mass $m_{tot} = m_1 + m_2 + m_3 + m_4 + m_5 + m_6 + m_7 + m_8$ and the equivalent masses $m_2^a = m_2(1 - e_2/l_2)$, $m_6^a = m_6(1 - p_6/a_2)$, and $m_6^b = m_6 p_6/a_2$.

In Fig. 14b the motion of the second DoF is illustrated where link 4 rotates about P_{43}, link 8 rotates about D_4, links 1, 3, and 7 have translational motion and link 5 is immobile. The linear momentum L_2 of this motion can be written with respect to reference frame x_2y_2, which is aligned with A_0A_3 as illustrated, and must be equal to the linear momentum of the total mass moving in S:

$$\frac{L_2}{\dot{\theta}_2} = \begin{bmatrix} -(m_1 + m_2^a)a_6 + m_4p_4 + m_8(a_4 - p_8) + \\ (m_2^b + m_3)(l_4 - a_6) + (m_6^a + m_7)a_4 \\ 0 \end{bmatrix} = \begin{bmatrix} m_{tot}a_4 \\ 0 \end{bmatrix} \tag{5}$$

with $m_2^b = m_2e_2/l_2$.

In Fig. 14c the motion of the third DoF is illustrated where link 3 rotates about A_3, link 7 rotates synchronously about B_6, and all other links are immobile. The linear momentum L_3 of this motion can be written with respect to reference frame x_3y_3, which is aligned with A_3A_2 as illustrated, and must be equal to the linear momentum of the total mass moving in S:

$$\frac{L_3}{\dot{\theta}_3} = \begin{bmatrix} m_2^b l_3 + m_3e_3 + m_7(a_3 - p_7) + m_6^a a_3 \\ 0 \end{bmatrix} = \begin{bmatrix} m_{tot}a_3 \\ 0 \end{bmatrix} \tag{6}$$

With the linear momentum equations (Eqs. 4–6) the second group of balance conditions is readily known. After substituting m_{tot}, they can be rewritten as:

$$(m_2 + m_3 + m_4)a_5 - m_1p_1 - m_2^a l_1 - m_5p_5 - m_6^b a_1 = 0 \tag{7}$$

$$\begin{aligned}(m_1 + m_2 + m_3 + m_4 + m_5 + m_6^b)a_4 + (m_1 + m_2 + m_3)a_6 \\ -(m_2^b + m_3)l_4 - m_4p_4 + m_8p_8 = 0\end{aligned} \tag{8}$$

$$(m_1 + m_2 + m_3 + m_4 + m_5 + m_6^b + m_8)a_3 - m_2^b l_3 - m_3e_3 + m_7p_7 = 0 \tag{9}$$

Table 2
Numerical example of parameter values for inherent balance of the TWIN-4B in Fig. 13.

(cm)	(kg)	(cm)	(cm)
$l_1 = 70$	$m_1 = 7.00$	$p_1 = 18.73$	$a_1 = 11.36$
$l_2 = 65$	$m_2 = 6.50$	$e_2 = 32.50$	$a_2 = 10.55$
$l_3 = 55$	$m_3 = 5.50$	$e_3 = 27.50$	$a_3 = 8.92$
$l_4 = 100$	$m_4 = 10.00$	$p_4 = 23.76$	$a_4 = 16.22$
	$m_5 = 2.76$	$p_5 = -2.45$	$a_5 = 16.27$
	$m_6 = 1.05$	$p_6 = 5.27$	$a_6 = 26.24$
	$m_7 = 0.89$	$p_7 = 4.46$	
	$m_8 = 4.25$	$p_8 = 21.23$	

By combining the kinematic balance conditions with these mass balance conditions the force balance conditions of the TWIN-4B in Fig. 13 are found as:

$$(m_2+m_3+m_4)a_5 - m_1p_1 - \left(m_2\left(1-\frac{e_2}{l_2}\right) + m_6\frac{p_6}{l_2}\right)l_1 - m_5p_5 = 0 \tag{10}$$

$$\begin{aligned}(m_1+m_2+m_3+m_4+m_5)a_4 + (m_1+m_2+m_3)a_6 \\ -\left(m_2\frac{e_2}{l_2} + m_3 - m_6\frac{p_6}{l_2}\right)l_4 - m_4p_4 + m_8p_8 = 0\end{aligned} \tag{11}$$

$$(m_1+m_2+m_3+m_4+m_5+m_8)\frac{l_3}{l_4}a_4 - \left(m_2\frac{e_2}{l_2} - m_6\frac{p_6}{l_2}\right)l_3 - m_3e_3 + m_7p_7 = 0 \tag{12}$$

where $a_2 = l_2a_1/l_1$, $a_2 = l_2a_4/l_4$, $a_2 = l_2a_3/l_3$ and $a_3 = l_3a_4/l_4$ were substituted together with the expressions for the equivalent masses m_2^a, m_2^b, m_6^a, and m_6^b.

When designing the linkage, it is possible to choose, for instance, the relative size of the similar four-bars with a scaling factor λ. Then $a_1 = \lambda l_1$, $a_2 = \lambda l_2$, $a_3 = \lambda l_3$, $a_4 = \lambda l_4$ and from the force balance conditions (10–12) parameters a_5, a_6, and p_7 can be calculated, respectively, as:

$$a_5 = \frac{m_1p_1 + m_2(1-\frac{e_2}{l_2})l_1 + m_5p_5 + m_6\frac{p_6}{l_2}l_1}{m_2+m_3+m_4} \tag{13}$$

$$a_6 = \frac{-(m_1+m_2+m_3+m_4+m_5)\lambda l_4 + (m_2\frac{e_2}{l_2} + m_3 - m_6\frac{p_6}{l_2})l_4 + m_4p_4 - m_8p_8}{m_1+m_2+m_3} \tag{14}$$

$$p_7 = \frac{-(m_1+m_2+m_3+m_4+m_5+m_8)\lambda l_3 + (m_2\frac{e_2}{l_2} - m_6\frac{p_6}{l_2})l_3 + m_3e_3}{m_7} \tag{15}$$

On the other hand it is also possible the leave the relative size of the similar four-bars dependent by calculating a_4 from (12) as:

$$a_4 = \frac{l_4}{l_3}\left(\frac{(m_2\frac{e_2}{l_2} - m_6\frac{p_6}{l_2})l_3 + m_3e_3 - m_7p_7}{m_1+m_2+m_3+m_4+m_5+m_8}\right) \tag{16}$$

The scaling factor of the similar four-bars then is determined by $\lambda = a_4/l_4$ with which a_1, a_2, a_3, a_5, and a_6 can be obtained as in the first case.

As a numerical example, Table 2 shows a set of parameter values for which the TWIN-4B is inherently balanced and S is the common CoM for any motion of the linkage. The results represent the realistic situation when the mass of each link is directly related to the length of each link (mass per length is equal for all links) and when the link CoM of each link is halfway the link. The scaling factor of the inner four-bar with respect to the outer four-bar here is $\lambda = 0.16$. It is possible to scale the linkage geometry without affecting the balance, i.e. all lengths in Table 2 could be multiplied by, for instance, seven or ten and the design would remain balanced with the same mass values. Similarly all mass values in Table 2 could be multiplied by any number without affecting the balance for the same geometry, link lengths and link CoM positions.

6. Synthesis example of a spatial inherently balanced double Bennett linkage

The principal vectors are not limited to planar motions: they describe the motion of the link CoMs with respect to the common CoM for any spatial motion. For instance, the four-bar linkage in Fig. 1a could have spherical joints in A_0, A_1, A_2, and A_3 and move out of plane with exactly the same principal vectors as for the planar case with revolute pairs. For spatial

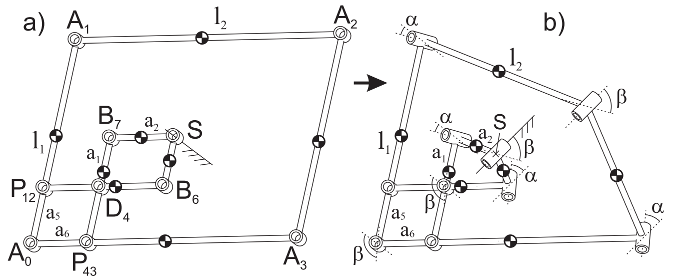

Fig. 15. The Inherently Balanced Double Bennett Linkage with its common CoM in fixed joint S (b) can be obtained from the planar TWIN-4B linkage by having equal opposite link lengths as in (a) and by twisting the revolute pairs out of plane according to the Bennett conditions.

Table 3
Numerical example of parameter values for inherent balance of the Double Bennett Linkage in Fig. 15.

(cm)	(kg)	(cm)	(cm)
$l_1 = 70$	$m_1 = 7.00$	$p_1 = 17.31$	$a_1 = 13.75$
$l_2 = 90$	$m_2 = 9.00$	$e_2 = 45.00$	$a_2 = 17.67$
$l_3 = l_1$	$m_3 = m_1$	$e_3 = 35.00$	$a_3 = a_1$
$l_4 = l_2$	$m_4 = m_2$	$p_4 = 22.43$	$a_4 = a_2$
	$m_5 = 3.14$	$p_5 = -1.97$	$a_5 = 17.69$
	$m_6 = 1.77$	$p_6 = 8.84$	$a_6 = 22.57$
	$m_7 = 1.37$	$p_7 = 6.87$	
	$m_8 = 4.02$	$p_8 = 20.12$	

motion the principal vectors define planes, the principal vector planes, with different orientations [36]. In fact, the planar situation is just a specific case of the general spatial situation when all the principal vectors are within the same plane and the different principal vector planes obtain the same orientation and unite to a single plane. This means that also the Grand Architecture in Fig. 3 can be transformed into a spatially moving inherently balanced linkage architecture. The challenge, however, is to find the right combination of joints to ensure the correct spatial motions, not gaining overmobility and on the other hand not locking the linkage immobile. It is beyond the scope of this article to study this in detail, but as an example with solely revolute pairs it is illustrated how the TWIN-4B linkage can be transformed into a spatial inherently balanced double Bennett linkage.

The Bennett linkage is a spatial four-bar linkage with solely revolute pairs as joints [37]. It is possible to change the two similar four-bars of the TWIN-4B linkage in Figs. 7a and 13a into two similar Bennett linkages by including the same Bennett conditions for each of them. Then the first step is to include the Bennett condition that opposite links have equal length, which is illustrated in Fig. 15a where $l_1 = l_3$, $l_2 = l_4$, $a_1 = a_3$, and $a_2 = a_4$. This results in a linkage with three parallelograms, one with sides l_1 and l_2, a similar one with sides a_1 and a_2, and a third one with sides a_5 and a_6. The next step is to include the twist angles of the axes of rotation of the joints, which are again equal for each pair of opposite links and are related with

$$\frac{\sin\alpha}{l_1} = \frac{\sin\beta}{l_2} \tag{17}$$

This is illustrated for $\alpha = 40^\circ$ and $\beta = 55.73^\circ$ in Fig. 15b which shows the resulting linkage with the two similar Bennett linkages. The parallelogram $A_0P_{12}D_4P_{43}$ remains planar and connects the two similar Bennetts such that they move similarly at all times. By including the Bennett conditions, the force balance conditions (10–12) do not change and determine the common CoM of this Inherently Balanced Double Bennett Linkage to be in (fixed) joint S for all motions. Table 3 shows a numerical example of a set of parameter values for inherent balance. Since the values do not depend on the twist angles, they hold for any twist of the four-bars. Similarly as for the TWIN-4B values in Table 2, also here the values represent the realistic situation shown in Fig. 15b where the mass of each link is directly related to the length of each link and where the link CoM of each link is halfway the link. Here the scaling factor of the inner Bennett with respect to the outer Bennett is $\lambda = 0.20$.

7. Discussion

The Grand Architecture in Fig. 3 was formed from four closed-chain principal vector linkages with some links extended to pivots C_i as illustrated in Fig. 2. Other link extensions with extra joints are also possible, for instance links $P_{21}B_1$ and $P_{42}B_5$ could be extended to a common joint forming a parallelogram with sides SB_1 and SB_5. This was shown in the solution in Fig. 5b where the new common joint is E_1. Four of these extra parallelograms are possible in the Grand Architecture, however they do not add new kinematic information. Essentially they just extend existing parallelograms and therefore they are only design variations as explained for Fig. 5. This is also true for the multitude of other possible parallelogram extensions which therefore are not included in the Grand Architecture.

These additional parallelograms however can be very useful in the synthesis of inherently balanced mechanisms. The inherently balanced linkage solutions presented in this paper are mainly a direct result of link elimination from the Grand Architecture. The solutions still can be modified in a variety of ways without losing their property of inherent balance. For instance by shifting or redesigning the parallelogram links and also by exchanging links with other mechanism elements such as gears and sliders. Also new links may be added that move similarly to other links in the Grand Architecture. As long as the kinematic properties of the Grand Architecture are maintained, any change is possible without disrupting the inherent balance. This next step in the synthesis is still a topic under investigation.

A disadvantage of the presented inherently balanced linkage solutions could be their limited range of motion due to singularities of the parallelograms. Exchanging links with other mechanism elements may be required to enlarge the range of motion. Also the choice of the closed-chain four-bar linkage as basis of the grand architecture limited the results that could be found to 2-DoF solutions. To find other solutions, for instance with 3-DoF or 4-DoF, other linkages need to be used as basis of a grand architecture with which the approach in this paper can be followed.

This paper does not consider the shaking moment balance, however inherently shaking moment-balanced mechanisms can be obtained from inherently force-balanced linkage solutions by reducing the DoFs of the force-balanced linkage solution. For instance from a 3-DoF force-balanced linkage solution a 2-DoF force- and moment-balanced linkage solution can be derived by constraining the relative motions according to the inertia parameters. This can be accomplished for instance by introducing slider elements [38].

Almost all inherently balanced linkage solutions in this paper were obtained by solely removing links from the inside of the Grand Architecture. This results in linkages that are force balanced without the need of countermasses, which is rare for common balance methods since for them the use of countermasses is the main issue. The link CoM of all links can be at or nearby their natural locations, which is perfectly according to the philosophy of *inherent balance*. When links of the circumscribed four-bar are eliminated instead of inner links, then linkage solutions are obtained with links that extend freely as shown for linkage solution 10 in the appendix. These extended links could be regarded as kind of countermasses, however they can also be applied as useful links in an application. This category of inherently balanced linkage solutions is left for future work.

All the inherently balanced linkage solutions consist of at least 8 links. For a parallel mechanism or robot manipulator design the solutions where two links are connected in the common CoM S is useful since then, to drive the 2-DoFs of the linkage, the two actuators can be mounted at the base. For other applications such as deployable structures it might be more practical to have a single link in S.

The force balance conditions showed to consist of two parts: (1) kinematic balance conditions given by the Grand Architecture and (2) mass balance conditions determining the mass parameter values of the links. This is different from common balance methods which only consider the second part. It is because of the kinematic balance conditions that advantageous balance solutions are obtained with the presented inherent balance approach.

It was shown that the solutions that can be derived from the Grand Architecture with mass asymmetric links in Fig. 9 is limited as compared to the solutions that can be derived from the Grand Architecture with mass symmetric links in Fig. 3. However, nothing restricts the designer to change the links of a mass symmetric inherently balanced linkage solution into mass asymmetric links, that's very well possible. Also then the mass balance conditions can be obtained from the linear momentum equations which for mass asymmetric links is more extensive as explained in [26].

From the result of the inherently balanced double Bennett linkage in Fig. 15b, together with the Grand Architecture in Fig. 3, it can be derived that the common CoM of a normal Bennett linkage traces a coupler curve of a similar Bennett linkage which is also similar to a coupler curve of the Bennett linkage itself. This is an extension of the theory of Kreutzinger explained in Section 3 which shows the same property for planar four-bar linkages [29]. It will be interesting to investigate this property also for other spatial inherently balanced linkage solutions.

8. Conclusions

In this paper the Grand 4R Four-Bar Based Inherently Balanced Linkage Architecture was presented and it was shown how from this highly overconstrained mechanism a variety of 32 normally constrained 2-DoF inherently balanced linkage solutions could be derived by removing specific combinations of redundant links. These solutions all have specific kinematic properties of similarity with advantageous balance capability such as no need of countermasses. For one linkage solution named the TWIN-4B it was shown how the balance conditions regarding the mass parameters can be derived with linear momentum equations and the balance conditions for all 32 solutions were presented. The difference between solutions with mass symmetric links and mass asymmetric links was explained. From the Grand Architecture with mass asymmetric links fewer solutions can be derived as compared to the Grand Architecture with mass symmetric links, while, interestingly, all the mass symmetric link solutions can also have mass asymmetric links. It was shown how a planar inherently balanced linkage solution could be transformed into a spatial inherently balanced linkage solution by example of the TWIN-4B which resulted, after including the Bennett conditions, into an inherently balanced double Bennett linkage. All these results together present a tool that allows designers to first select an inherently balanced linkage solution as their starting point in the design of their balanced device, which is expected to be significantly more fruitful than trying to balance a certain linkage at the end.

Declaration of Competing Interest

The authors declare that they have no known competing financial interests or personal relationships that could have appeared to influence the work reported in this paper.

Acknowledgment

This publication was financially supported by the Netherlands Organisation for Scientific Research (NWO, NWO15146).

Appendix: Overview of 2-DoF inherently balanced linkages with their conditions for shaking force balance and gravity force balance

This appendix presents 32 2-DoF inherently balanced linkage solutions with mass symmetric links derived from the Grand Architecture in Fig. 3 together with their balance conditions. The mass balance conditions are comparable to and derived as Eqs. (7)–(9) in Section 5, which are without the kinematic balance conditions. The kinematic balance conditions which determine the similar motions of parallel links and the similarity of four-bars are given for all linkage solutions in Table 4. As such, the designer can directly use each of these 32 linkages as a starting point in their design of a force balanced device.

Inherently balanced linkage		Mass balance conditions
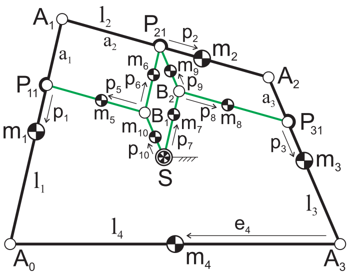	1	$(m_2+m_3+m_4+m_8+m_9)a_1-$ $m_1p_1-m_4\frac{e_4}{l_4}l_1+m_6p_6+m_7p_7=0$ $(m_1+m_3+m_4)a_2-m_2p_2+m_5p_5-$ $(m_3+m_4(1-\frac{e_4}{l_4}))l_2-m_8p_8=0$ $(m_1+m_2+m_4+m_5+m_6)a_3-m_3p_3-$ $m_4(1-\frac{e_4}{l_4})l_3+m_9p_9+m_{10}p_{10}=0$
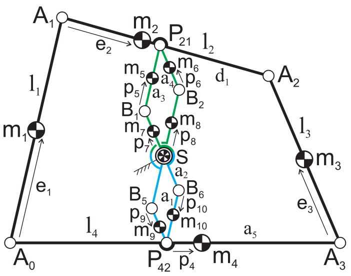	2	$(m_1+m_2+m_3+m_4+m_9)a_1-$ $m_1e_1-m_2(1-\frac{e_2}{l_2})l_1-m_5p_5-$ $m_6a_3-m_8p_8+m_{10}p_{10}=0$ $(m_1+m_2+m_3)a_5+m_4p_4-$ $(m_1+m_2(1-\frac{e_2}{l_2}))l_4=0$ $(m_1+m_2+m_3+m_4+m_{10})a_2-$ $m_3e_3-m_2\frac{e_2}{l_2}l_3-m_5a_4-$ $m_6p_6-m_7p_7+m_9p_9=0$
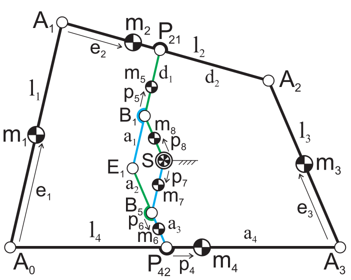	3	$(m_1+m_2+m_3+m_4+m_6)a_1-$ $m_1e_1-m_2(1-\frac{e_2}{l_2})l_1-m_5p_5+$ $m_7p_7=0$ $(m_1+m_2+m_3)a_4+m_4p_4-$ $(m_1+m_2(1-\frac{e_2}{l_2}))l_4=0$ $(m_1+m_2+m_3+m_4)a_3-m_3e_3-$ $m_2\frac{e_2}{l_2}l_3-m_5a_2+m_6p_6-m_8p_8=0$

(*continued on next page*)

Inherently balanced linkage		Mass balance conditions
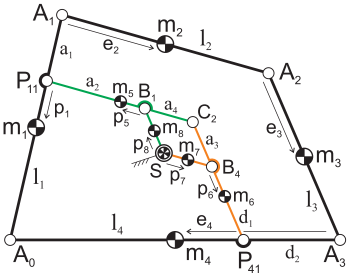	4	$(m_2+m_3+m_4)a_1-m_1p_1-m_4\frac{e_4}{l_4}l_1=0$ $(m_1+m_2+m_3+m_4)a_2-m_2e_2-(m_3+m_4(1-\frac{e_4}{l_4}))l_2+m_5p_5-m_6a_4-m_7p_7=0$ $(m_1+m_2+m_3+m_4+m_5)a_3-m_3e_3-m_4(1-\frac{e_4}{l_4})l_3-m_6p_6+m_8p_8=0$
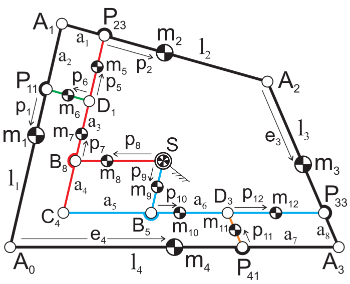	5	$(m_1+m_3+m_4+m_{11}(1-\frac{p_{11}}{a_8}))a_1-m_2p_2-m_3(1-\frac{e_3}{l_3})l_2+m_6p_6=0$ $(m_1+m_2+m_3+m_4+m_5+m_6+m_{11}(1-\frac{p_{11}}{a_8}))a_3-m_1p_1+m_5p_5+m_7p_7+(m_2+m_3+m_4+m_{11}(1-\frac{p_{11}}{a_8}))a_2-(m_3\frac{e_3}{l_3}+m_4+m_{11}(1-\frac{p_{11}}{a_8}))l_1-m_9p_9-(m_{10}+m_{11}\frac{p_{11}}{a_8}+m_{12})a_4=0$ $(m_1+m_2+m_3+m_4+m_5+m_6+m_7+m_{11}(1-\frac{p_{11}}{a_8}))a_5-m_4e_4-m_3\frac{e_3}{l_3}l_4-m_{11}(1-\frac{p_{11}}{a_8})(l_4-a_7)-m_{10}p_{10}-m_{11}\frac{p_{11}}{a_8}a_6-m_{12}(a_6+p_{12})+m_8p_8=0$
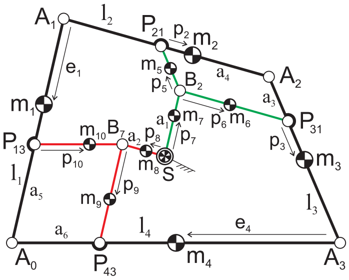	6	$(m_1+m_2+m_3+m_4+m_5+m_6+m_{10}(1-\frac{p_{10}}{a_6}))a_1-m_1e_1+m_7p_7-(m_4\frac{e_4}{l_4}+m_{10}(1-\frac{p_{10}}{a_6}))l_1-m_9p_9+m_{10}(1-\frac{p_{10}}{a_6})a_5=0$ $(m_1+m_3+m_4+m_{10}(1-\frac{p_{10}}{a_6}))a_4-(m_1+m_4\frac{e_4}{l_4}+m_{10}(1-\frac{p_{10}}{a_6}))l_2+m_2p_2+m_6p_6-m_8p_8-(m_9+m_{10}\frac{p_{10}}{a_6})a_2=0$ $(m_1+m_2+m_4+m_{10}(1-\frac{p_{10}}{a_6}))a_3-m_3p_3-m_4(1-\frac{e_4}{l_4})l_3+m_5p_5=0$
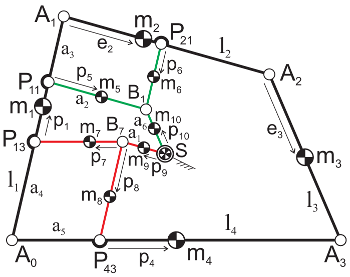	7	$(m_1+m_2+m_3+m_4+m_5+m_6+m_7+m_8+m_{10}\frac{p_{10}}{a_6})a_1-m_2e_2-m_3(1-\frac{e_3}{l_3})l_2-m_5p_5-(m_6+m_{10}\frac{p_{10}}{a_6})a_2+m_9p_9=0$ $(m_2+m_3+m_4+m_5+m_6+m_{10}\frac{p_{10}}{a_6})a_4-(m_2+m_3(1-\frac{e_3}{l_3})+m_5+m_6+m_{10}\frac{p_{10}}{a_6})l_1-m_1p_1+(m_5+m_{10}\frac{p_{10}}{a_6})a_3+m_6p_6+m_8p_8=0$ $(m_1+m_2+m_3+m_5+m_6+m_{10}\frac{p_{10}}{a_6})a_5-m_4p_4-m_3\frac{e_3}{l_3}l_4+m_7p_7=0$
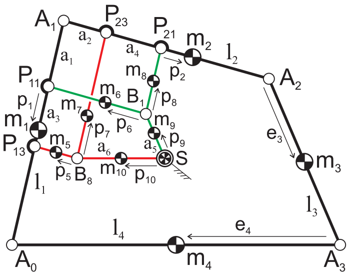	8	$(m_2+m_3+m_4)a_1-m_1p_1-m_4\frac{e_4}{l_4}l_1-(m_5+m_7+m_{10}\frac{p_{10}}{a_6})a_3+m_7p_7+m_8p_8=0$ $m_2p_2+(m_3+m_4(1-\frac{e_4}{l_4}))l_2-(m_1+m_3+m_4)a_2-(m_1+m_3+m_4+m_5+m_7+m_{10}\frac{p_{10}}{a_6})a_4-m_5p_5-m_6p_6=0$ $(m_1+m_2+m_3+m_4+m_5+m_6+m_7+m_8+m_{10}\frac{p_{10}}{a_6})a_5-m_3e_3-m_4(1-\frac{e_4}{l_4})l_3+m_9p_9=0$

(continued on next page)

Inherently balanced linkage		Mass balance conditions
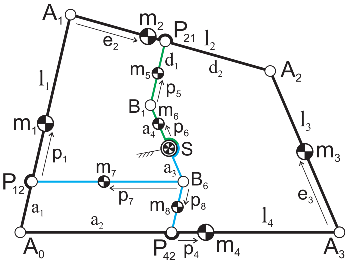	9	$(m_2+m_3+m_4)a_1 - m_2(1-\frac{e_2}{l_2})l_1 - m_1p_1 - m_5p_5 + m_8p_8 = 0$ $(m_1+m_2+m_3)a_2 - m_4p_4 - (m_2\frac{e_2}{l_2}+m_3)l_4 + m_7p_7 = 0$ $(m_1+m_2+m_3+m_4+m_7+m_8)a_3 - m_2\frac{e_2}{l_2}l_3 - m_3e_3 - m_5a_4 - m_6p_6 = 0$
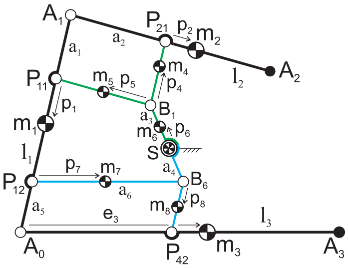	10	$(m_2+m_3(1-\frac{e_3}{a_6})+m_7(1-\frac{p_7}{a_6}))a_1 - m_1p_1 - m_3(1-\frac{e_3}{a_6})l_1 - m_3\frac{e_3}{a_6}a_5 + m_4p_4 - m_7(1-\frac{p_7}{a_6})(l_1-a_5) - m_8p_8 = 0$ $(m_1+m_3(1-\frac{e_3}{a_6})+m_7(1-\frac{p_7}{a_6}))a_2 - m_2p_2 + m_5p_5 = 0$ $(m_1+m_2+m_3(1-\frac{e_3}{a_6})+m_4+m_5+m_7(1-\frac{p_7}{a_6}))a_3 + m_6p_6 - (m_3\frac{e_3}{a_6}+m_7\frac{p_7}{a_6}+m_8)a_4 = 0$
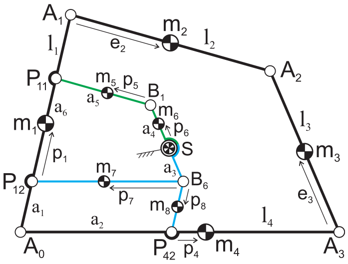	11	$(m_2+m_3+m_4)a_1 - m_5\frac{p_5}{a_5}a_6 - m_1p_1 - m_2(1-\frac{e_2}{l_2})l_1 + m_8p_8 = 0$ $(m_1+m_2+m_3+m_5\frac{p_5}{a_5})a_2 - m_4p_4 - (m_2\frac{e_2}{l_2}+m_3)l_4 + m_7p_7 = 0$ $(m_1+m_2+m_3+m_4+m_5\frac{p_5}{a_5}+m_7+m_8)a_3 - m_2\frac{e_2}{l_2}l_3 - m_3e_3 - m_5(1-\frac{p_5}{a_5})a_4 - m_6p_6 = 0$
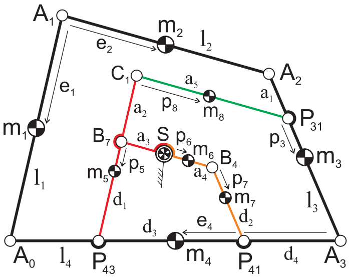	12	$(m_1+m_2+m_3+m_4+m_8)a_2 - m_1e_1 - m_4\frac{e_4}{l_4}l_1 - m_5p_5 = 0$ $(m_1+m_2+m_3+m_4+m_5+m_8)a_3 - (m_1+m_2+m_3+m_4)a_5 + (m_1+m_2+m_4\frac{e_4}{l_4})l_2 - m_2e_2 - m_6p_6 - m_7a_4 - m_8p_8 = 0$ $(m_1+m_2+m_4)a_1 - m_3p_3 - m_4(1-\frac{e_4}{l_4})l_3 - m_7p_7 = 0$
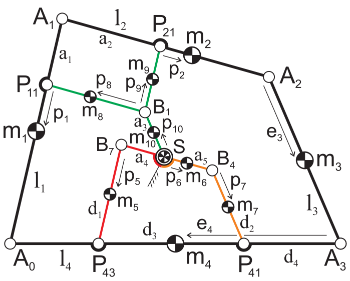	13	$(m_2+m_3+m_4)a_1 - m_1p_1 - m_4\frac{e_4}{l_4}l_1 + m_9p_9 - m_5p_5 = 0$ $m_2p_2 + m_6p_6 - m_8p_8 - m_5a_4 - (m_1+m_3+m_4)a_2 + m_7a_5 + (m_3+m_4(1-\frac{e_4}{l_4}))l_2 = 0$ $(m_1+m_2+m_3+m_4+m_8+m_9)a_3 - m_3e_3 - m_4(1-\frac{e_4}{l_4})l_3 - m_7p_7 + m_{10}p_{10} = 0$

(continued on next page)

Inherently balanced linkage		Mass balance conditions
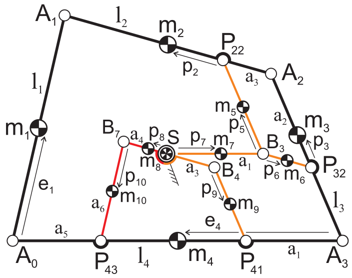	14	$(m_1+m_2+m_3+m_4+m_5+m_6+m_{10}\frac{p_{10}}{a_6})a_1-(m_1(1-\frac{e_1}{l_1})+m_{10}\frac{p_{10}}{a_6})l_4-m_4e_4+m_7p_7+m_{10}\frac{p_{10}}{a_6}a_5=0$ $(m_1+m_2+m_4+m_{10}\frac{p_{10}}{a_6})a_2+m_3p_3-(m_1(1-\frac{e_1}{l_1})+m_4+m_{10}\frac{p_{10}}{a_6})l_3+m_5p_5-m_9p_9=0$ $(m_1+m_3+m_4+m_9+m_{10}\frac{p_{10}}{a_6})a_3-m_1\frac{e_1}{l_1}l_2-m_2p_2+m_6p_6-m_8p_8-m_{10}(1-\frac{p_{10}}{a_6})a_4=0$
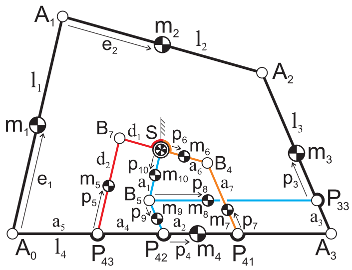	15	$(m_1+m_2+m_3+m_4+m_5+m_6\frac{p_6}{a_6}+m_7+m_8+m_9)a_1-m_1e_1-m_2(1-\frac{e_2}{l_2})l_1-m_5p_5+m_{10}p_{10}=0$ $(m_1+m_2+m_3+m_5)a_4-(m_6\frac{p_6}{a_6}+m_7)a_2+(m_1+m_2+m_3)a_5-(m_2\frac{e_2}{l_2}+m_3)l_4-m_4p_4-m_8p_8=0$ $(m_1+m_2+m_4+m_5+m_6\frac{p_6}{a_6}+m_7)a_3-m_2\frac{e_2}{l_2}l_3-m_3p_3-m_6\frac{p_6}{a_6}a_7-m_7p_7+m_9p_9=0$
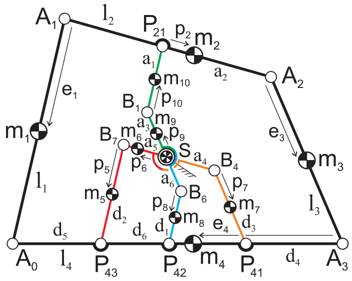	16	$(m_1+m_2+m_3+m_4)a_1-m_1e_1-m_4\frac{e_4}{l_4}l_1-m_5p_5-m_8p_8+m_{10}p_{10}=0$ $(m_1+m_3+m_4)a_2+m_2p_2-(m_1+m_4\frac{e_4}{l_4})l_2-m_5a_5-m_6p_6+m_7a_4=0$ $(m_1+m_2+m_3+m_4+m_{10})a_3-m_3e_3-m_4(1-\frac{e_4}{l_4})l_3-m_7p_7-m_8a_6+m_9p_9=0$
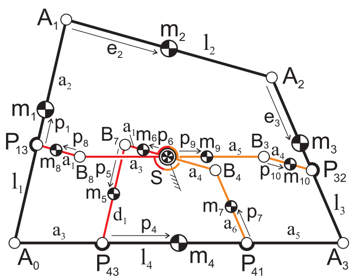	17	$(m_1+m_2+m_3+m_4+m_5+m_7(1-\frac{p_7}{a_6}))a_1-m_3(1-\frac{e_3}{l_3})l_2-m_2e_2+m_6p_6-m_7\frac{p_7}{a_6}a_4+m_8p_8-m_{10}p_{10}=0$ $(m_2+m_3+m_4+m_7(1-\frac{p_7}{a_6}))a_2-(m_3\frac{e_3}{l_3}+m_4+m_7(1-\frac{p_7}{a_6}))l_1+m_1p_1-m_5p_5=0$ $(m_1+m_2+m_3+m_7(1-\frac{p_7}{a_6})+m_8)a_3-(m_3\frac{e_3}{l_3}+m_7(1-\frac{p_7}{a_6}))l_4-m_4p_4+(m_7(1-\frac{p_7}{a_6})-m_{10})a_5-m_9p_9=0$
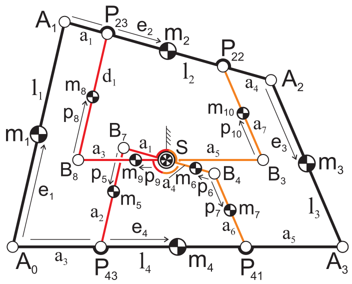	18	$(m_1+m_2+m_3+m_4+m_5+m_7\frac{p_7}{a_6}+m_{10}\frac{p_{10}}{a_7})a_1-m_2e_2-(m_3(1-\frac{e_3}{l_3})+m_{10}\frac{p_{10}}{a_7})l_2-(m_6+m_7(1-\frac{p_7}{a_6})-m_{10}\frac{p_{10}}{a_7})a_4+m_6p_6=0$ $(m_1+m_2+m_3+m_4+m_7\frac{p_7}{a_6}+m_{10}\frac{p_{10}}{a_7})a_2-m_1e_1-(m_2+m_3(1-\frac{e_3}{l_3})+m_{10}\frac{p_{10}}{a_7})l_1+m_5p_5-m_8p_8=0$ $(m_1+m_2+m_3+m_4+m_7\frac{p_7}{a_6}+m_8+m_{10}\frac{p_{10}}{a_7})a_3-m_4e_4-(m_3\frac{e_3}{l_3}+m_7\frac{p_7}{a_6})l_4+m_9p_9+(m_7\frac{p_7}{a_6}-m_{10}(1-\frac{p_{10}}{a_7}))a_5=0$

(continued on next page)

Inherently balanced linkage		Mass balance conditions
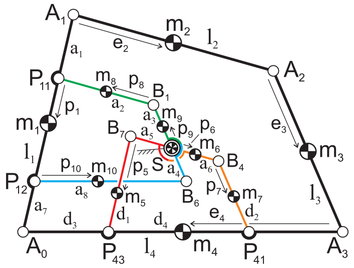	19	$(m_2+m_3+m_4+m_{10}(1-\frac{p_{10}}{a_8}))a_1-m_1p_1-(m_4\frac{e_4}{l_4}+m_{10}(1-\frac{p_{10}}{a_8}))l_1-m_5p_5+m_{10}(1-\frac{p_{10}}{a_8})a_7=0$ $(m_1+m_2+m_3+m_4+m_{10}(1-\frac{p_{10}}{a_8}))a_2-m_2e_2-(m_3+m_4(1-\frac{e_4}{l_4}))l_2+m_5a_5-m_6p_6-m_7a_6+m_8p_8=0$ $(m_1+m_2+m_3+m_4+m_8+m_{10}(1-\frac{p_{10}}{a_8}))a_3-m_3e_3-m_4(1-\frac{e_4}{l_4})l_3-m_7p_7+m_9p_9-m_{10}\frac{p_{10}}{a_8}a_4=0$
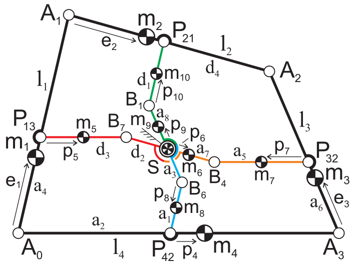	20	$(m_1+m_2+m_3+m_4+m_5+m_6\frac{p_6}{a_7}+m_7)a_1-m_1e_1-m_2(1-\frac{e_2}{l_2})l_1-m_5a_4+m_8p_8-m_{10}p_{10}=0$ $(m_1+m_2+m_3+m_5+m_6\frac{p_6}{a_7}+m_7)a_2-(m_2\frac{e_2}{l_2}+m_3+m_6\frac{p_6}{a_7}+m_7)l_4-m_4p_4-m_5p_5+m_6\frac{p_6}{a_7}a_5+m_7p_7=0$ $(m_1+m_2+m_3+m_4+m_5+m_6\frac{p_6}{a_7}+m_7+m_8)a_3-m_2\frac{e_2}{l_2}l_3-m_3e_3-(m_6\frac{p_6}{a_7}+m_7)a_6-m_9p_9-m_{10}a_8=0$
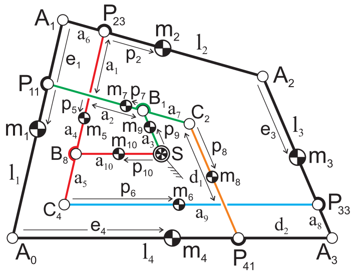	21	Same conditions as for 22
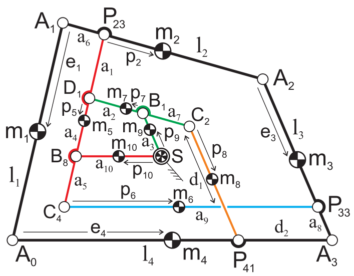	22	$(m_1+m_2+m_3+m_4+m_6\frac{p_6}{a_9})a_1-m_1e_1-m_4(1-\frac{e_4}{l_4})l_1-m_5p_5-m_6(1-\frac{p_6}{a_9})(a_4+a_5)-m_{10}\frac{p_{10}}{a_{10}}a_4=0$ $(m_1+m_2+m_3+m_4+m_5+m_6+m_{10}\frac{p_{10}}{a_{10}})a_2+(m_1+m_3+m_4+m_6\frac{p_6}{a_9})a_6-m_2p_2-(m_3+m_4\frac{e_4}{l_4}+m_6\frac{p_6}{a_9})l_2+m_7p_7-m_8a_7=0$ $(m_1+m_2+m_3+m_4+m_5+m_6+m_7+m_8+m_{10}\frac{p_{10}}{a_{10}})a_3-m_3e_3-(m_4\frac{e_4}{l_4}+m_6\frac{p_6}{a_9})l_3+m_6\frac{p_6}{a_9}a_8-m_8p_8+m_9p_9=0$
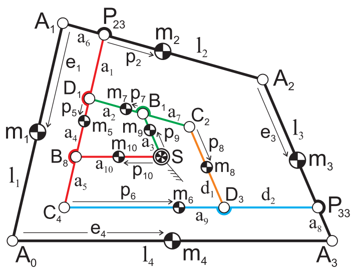	23	Same conditions as for 22

(continued on next page)

Inherently balanced linkage		Mass balance conditions
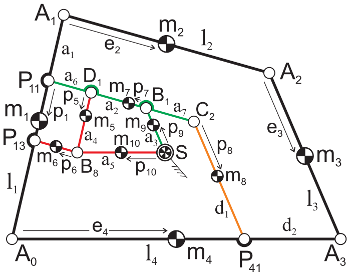	24	$(m_2+m_3+m_4)a_1 - m_1p_1 - m_4(1-\frac{e_4}{l_4})l_1 - m_5p_5 - (m_6+m_{10}\frac{p_{10}}{a_5})a_4 = 0$ $(m_1+m_2+m_3+m_4+m_5+m_6+m_{10}\frac{p_{10}}{a_5})a_2 + (m_1+m_2+m_3+m_4)a_6 - m_2e_2 - (m_3+m_4\frac{e_4}{l_4})l_2 + m_6p_6 + m_7p_7 - m_8a_7 = 0$ $(m_1+m_2+m_3+m_4+m_5+m_6+m_7+m_8+m_{10}\frac{p_{10}}{a_5})a_3 - m_3e_3 - m_4\frac{e_4}{l_4}l_3 - m_8p_8 + m_9p_9 = 0$
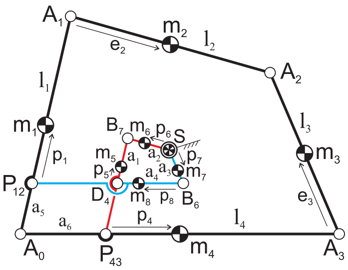	25	$(m_2+m_3+m_4)a_5 - m_1p_1 - m_2(1-\frac{e_2}{l_2})l_1 - m_5p_5 - m_6\frac{p_6}{a_2}a_1 = 0$ $(m_1+m_2+m_3+m_4+m_5+m_6\frac{p_6}{a_2})a_4 + (m_1+m_2+m_3)a_6 - (m_2\frac{e_2}{l_2}+m_3)l_4 - m_4p_4 + m_8p_8 = 0$ $(m_1+m_2+m_3+m_4+m_5+m_6\frac{p_6}{a_2}+m_8)a_3 - m_2\frac{e_2}{l_2}l_3 - m_3e_3 + m_7p_7 = 0$
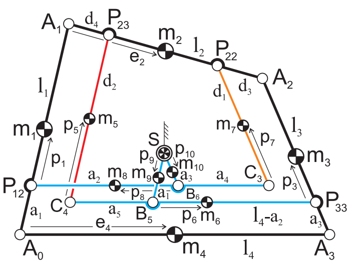	26	$(m_2+m_3+m_4+m_5+m_6)a_1 - m_1p_1 - m_2(1-\frac{e_2}{l_2})l_1 - m_5p_5 + m_9p_9 = 0$ $(m_1+m_2+m_3+m_4)a_2 - (m_2\frac{e_2}{l_2}+m_3)l_4 - m_4e_4 + m_5a_5 - m_6p_6 - m_7a_4 + m_8p_8 = 0$ $(m_1+m_2+m_4+m_7+m_8)a_3 - m_2\frac{e_2}{l_2}l_3 - m_3p_3 - m_7p_7 + m_{10}p_{10} = 0$
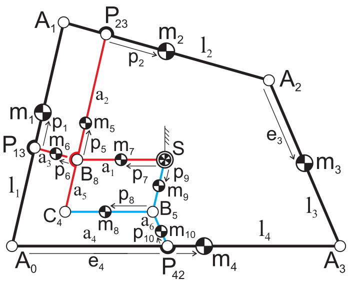	27	$(m_1+m_2+m_3+m_4+m_5+m_6+m_{10}(1-\frac{p_{10}}{a_6}))a_1 - m_4e_4 - m_3\frac{e_3}{l_3}l_4 + m_7p_7 + m_8p_8 - m_{10}(1-\frac{p_{10}}{a_6})a_4 = 0$ $(m_2+m_3+m_4+m_{10}(1-\frac{p_{10}}{a_6}))a_2 - (m_8+m_{10}\frac{p_{10}}{a_6})a_5 + m_1p_1 + m_5p_5 - (m_3\frac{e_3}{l_3}+m_4+m_{10}(1-\frac{p_{10}}{a_6}))l_1 - m_9p_9 = 0$ $(m_1+m_3+m_4+m_{10}(1-\frac{p_{10}}{a_6}))a_3 - m_2p_2 - m_3(1-\frac{e_3}{l_3})l_2 + m_6p_6 = 0$
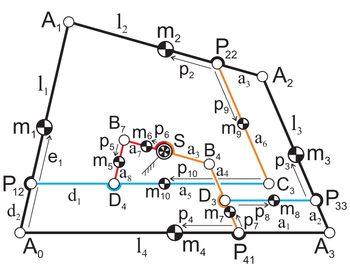	28	$(m_1+m_2+m_3+m_5\frac{p_5}{a_8}+m_9+m_{10})a_1 - m_1(1-\frac{e_1}{l_1})l_4 - m_4p_4 - m_5\frac{p_5}{a_8}a_5 + m_8p_8 - m_{10}p_{10} = 0$ $(m_1+m_2+m_3+m_4+m_5\frac{p_5}{a_8}+m_7+m_8+m_9+m_{10})a_4 + (m_1+m_2+m_4+m_5\frac{p_5}{a_8}+m_7+m_9+m_{10})a_2 - (m_1\frac{e_1}{l_1}+m_2+m_5\frac{p_5}{a_8}+m_9+m_{10})l_3 - m_3p_3 + (m_5\frac{p_5}{a_8}+m_{10})a_6 - m_7p_7 + m_9p_9 = 0$ $(m_1+m_3+m_4+m_7+m_8)a_3 - m_1\frac{e_1}{l_1}l_2 - m_2p_2 - m_5(1-\frac{p_5}{a_8})a_7 - m_6p_6 = 0$

(*continued on next page*)

Inherently balanced linkage		Mass balance conditions
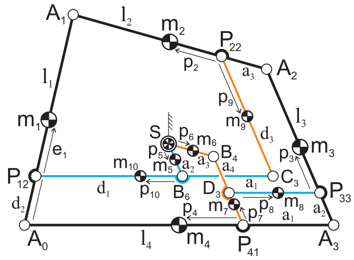	29	$(m_1+m_2+m_3+m_9)a_1-m_4p_4-m_1(1-\frac{e_1}{l_1})l_4+m_8p_8-m_{10}p_{10}=0$ $(m_1+m_2+m_4+m_7+m_9+m_{10})a_2+(m_1+m_2+m_3+m_4+m_7+m_8+m_9)a_4-m_3p_3-(m_1\frac{e_1}{l_1}+m_2+m_9)l_3+m_5p_5-m_7p_7+m_9p_9=0$ $(m_1+m_3+m_4+m_7+m_8)a_3-m_1\frac{e_1}{l_1}l_2-m_2p_2+m_6p_6=0$
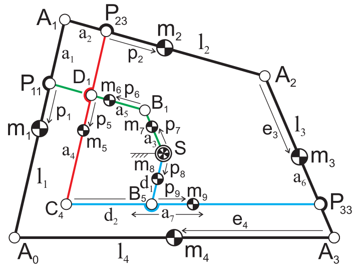	30	$(m_2+m_3+m_4+m_9\frac{p_9}{a_7})a_1-m_1p_1-m_4\frac{e_4}{l_4}l_1-m_5p_5-m_8p_8-m_9(1-\frac{p_9}{a_7})a_4=0$ $(m_1+m_3+m_4+m_9\frac{p_9}{a_7})a_2+(m_1+m_2+m_3+m_4+m_5+m_9)a_5-(m_3+m_4(1-\frac{e_4}{l_4})+m_9\frac{p_9}{a_7})l_2-m_2p_2+m_6p_6=0$ $(m_1+m_2+m_3+m_4+m_5+m_6+m_9)a_3-m_3e_3-m_4(1-\frac{e_4}{l_4})l_3+m_7p_7-m_9\frac{p_9}{a_7}a_6=0$
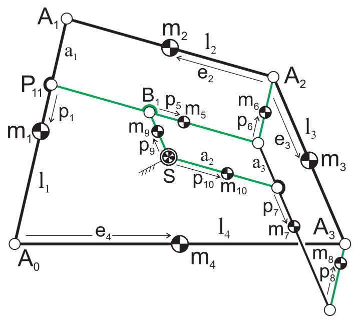	31	$(m_2+m_3+m_4)a_1-m_1p_1-m_4(1-\frac{e_4}{l_4})l_1+m_6p_6+m_8p_8=0$ $(m_1+m_2+m_3+m_4+m_6+m_7+m_8)a_2-(m_1+m_4(1-\frac{e_4}{l_4}))l_2-m_2e_2+m_5p_5+m_{10}p_{10}=0$ $(m_1+m_2+m_3+m_4+m_5+m_6+m_8)a_3-m_3e_3-(m_4\frac{e_4}{l_4}+m_8)l_3-m_7p_7+m_9p_9=0$
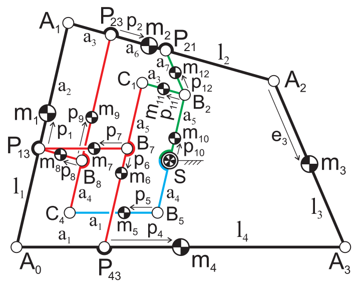	32	$(m_1+m_2+m_3+m_8+m_9+m_{12}\frac{p_{12}}{a_7})a_1-m_3\frac{e_3}{l_3}l_4-m_4p_4+m_5p_5+m_7p_7=0$ $(m_2+m_3+m_4+m_{12}\frac{p_{12}}{a_7})a_2+(m_{11}+m_{12}(1-\frac{p_{12}}{a_7}))a_5-(m_3\frac{e_3}{l_3}+m_4)l_1+m_1p_1-m_5a_4-m_6p_6+m_9p_9+m_{10}p_{10}=0$ $(m_1+m_3+m_4+m_6+m_7)a_3-m_2p_2-m_3(1-\frac{e_3}{l_3})l_2+m_8p_8+m_{11}p_{11}-m_{12}\frac{p_{12}}{a_7}a_6=0$

Table 4
Kinematic balance conditions of the 32 inherently balanced linkage solutions.

Linkage	Kinematic balance conditions
1	none
2	$\frac{a_1+a_3}{l_1}=\frac{a_5}{l_4}=\frac{d_1}{l_2},\ \frac{a_2+a_4}{l_3}=\frac{l_4-a_5}{l_4}$
3	$\frac{a_2+a_3}{l_3}=\frac{l_4-a_4}{l_4},\ \frac{a_4}{l_4}=\frac{a_1+d_1}{l_1}=\frac{d_2}{l_2}$
4	$\frac{l_1-a_1}{l_1}=\frac{a_2+a_4}{l_2}=\frac{a_3+d_1}{l_3}=\frac{l_4-d_2}{l_4}$
5	$\frac{a_1}{l_2}=\frac{a_8}{l_3},\ \frac{a_3}{l_1}=\frac{a_5}{l_4},\ \frac{a_2}{l_1}=\frac{a_7}{l_4},\ \frac{a_4}{l_1}=\frac{a_6}{l_4}=\frac{l_1-a_2-a_3}{l_1}-\frac{a_8}{l_3}$
6	$\frac{a_1+a_5}{l_1}=\frac{a_2+a_4}{l_2}=\frac{l_3-a_3}{l_3}=\frac{l_4-a_6}{l_4}$
7	$\frac{a_2-a_1}{l_2}=\frac{l_1-a_4-a_3}{l_1}=\frac{a_5}{l_4}=\frac{a_6}{l_3}$
8	$\frac{a_3}{l_1}=\frac{a_4}{l_2}=\frac{a_5}{l_3}=\frac{a_6}{l_4}$
9	$\frac{a_2}{l_4}=\frac{a_3+a_4}{l_3}=\frac{l_2-d_2}{l_2},\ \frac{l_4-a_2}{l_4}=\frac{a_1+d_1}{l_1}$

(continued on next page)

Table 4 (*continued*)

Linkage	Kinematic balance conditions
10	none
11	$\frac{a_2}{l_4}=\frac{a_3+a_4}{l_3}=\frac{a_5}{l_2}=\frac{a_6}{l_1}$
12	$\frac{l_3-a_1}{l_3}=\frac{a_5}{l_2}=\frac{d_1+a_2}{l_1}=\frac{d_3+d_4}{l_4},\ \frac{a_3+a_4}{l_2}=\frac{d_1}{l_1}=\frac{d_2}{l_3}=\frac{d_3}{l_4}$
13	$\frac{a_2-a_4}{l_2}=\frac{a_3}{l_3},\ \frac{a_1}{l_1}=\frac{l_2-a_2-a_5}{l_2}=\frac{d_4}{l_4},\ \frac{a_4+a_5}{l_2}=\frac{d_1}{l_1}=\frac{d_2}{l_3}=\frac{d_3}{l_4}$
14	$\frac{l_4-a_1-a_5}{l_4}=\frac{l_3-a_2}{l_3}=\frac{a_3+a_4}{l_2}=\frac{a_6}{l_1}$
15	$\frac{a_1}{l_1}=\frac{a_2}{l_4}=\frac{a_6}{l_2}=\frac{a_7-a_3}{l_3},\ \frac{a_2+a_4}{l_4}=\frac{a_7}{l_3}=\frac{d_1+a_6}{l_2}=\frac{d_2}{l_1}$
16	$\frac{a_1}{l_1}=\frac{a_2-a_4}{l_2}=\frac{d_4}{l_4},\ \frac{a_3}{l_3}=\frac{l_2-a_2-a_5}{l_2}=\frac{d_5}{l_4},\ \frac{a_5}{l_2}=\frac{a_6}{l_3}=\frac{d_6}{l_4}$ $\frac{l_2-a_2}{l_2}=\frac{a_3+a_6}{l_3},\ \frac{a_4}{l_2}=\frac{d_1}{l_1},\ \frac{a_4+a_5}{l_2}=\frac{d_2}{l_1}=\frac{d_3}{l_3}$
17	$\frac{a_1+a_4}{l_2}=\frac{l_1-a_2}{l_1}=\frac{l_4-a_3-a_5}{l_4}=\frac{a_6}{l_3}=\frac{d_1}{l_1}$
18	$\frac{a_1+a_4}{l_2}=\frac{a_2}{l_1}=\frac{a_6}{l_3},\ \frac{a_3+a_5}{l_4}=\frac{a_7}{l_3}=\frac{d_1}{l_1},\ a_7=l_3-a_6$
19	$\frac{l_1-a_1-a_7}{l_1}=\frac{a_2}{l_2}=\frac{a_3+a_4}{l_3}=\frac{a_8}{l_4},\ \frac{a_4}{l_3}=\frac{a_5}{l_2}=\frac{a_8-d_3}{l_4}$ $\frac{a_6}{l_2}=\frac{a_7}{l_1},\ \frac{a_5+a_6}{l_2}=\frac{d_1}{l_1}=\frac{d_2}{l_3}=\frac{d_4}{l_4}$
20	$\frac{a_1}{l_1}=\frac{l_4-a_2-a_5}{l_4}=\frac{a_6-a_3}{l_3}=\frac{a_7}{l_2},\ \frac{a_4-a_1}{l_1}=\frac{a_3}{l_3}=\frac{d_2}{l_2}=\frac{a_2-d_3}{l_4}$ $\frac{a_2}{l_4}=\frac{a_3+a_8}{l_3},\ \frac{a_5}{l_4}=\frac{d_1}{l_1}=\frac{d_4-a_7}{l_2}$
21	$\frac{a_1+a_4+a_5}{l_1}=\frac{l_2-a_6}{l_2}=\frac{l_3-a_8}{l_3}=\frac{a_9}{l_4},\ \frac{a_2}{l_2}=\frac{a_3}{l_3}=\frac{a_4}{l_1}=\frac{a_{10}}{l_4},$ $\frac{l_1-a_1}{l_1}=\frac{a_2+a_6+a_7}{l_2}=\frac{d_1+a_8}{l_3}=\frac{l_4-d_2}{l_4}$
22	equal to 21
23	equal to 21
24	$\frac{l_1-a_1}{l_1}=\frac{a_2+a_6+a_7}{l_2}=\frac{d_1}{l_3}=\frac{l_4-d_2}{l_4},\ \frac{a_2}{l_2}=\frac{a_3}{l_3}=\frac{a_4}{l_1}=\frac{a_5}{l_4}$
25	$\frac{a_1}{l_1}=\frac{a_2}{l_2}=\frac{a_3}{l_3}=\frac{a_4}{l_4}$
26	$\frac{l_1-a_1}{l_1}=\frac{a_2+a_4}{l_4}=\frac{d_1}{l_3}=\frac{l_2-d_3}{l_2},\ \frac{l_3-a_3}{l_3}=\frac{l_4-a_2+a_5}{l_4}=\frac{d_2}{l_1}=\frac{l_2-d_4}{l_2}$
27	$\frac{a_1+l_4-a_4}{l_4}=\frac{a_2+a_5}{l_1}=\frac{l_2-a_3}{l_2}=\frac{l_3-a_6}{l_3}$
28	$\frac{a_2}{l_3}=\frac{a_7}{l_2}=\frac{a_8}{l_1},\ \frac{a_3}{l_2}=\frac{a_4}{l_3}=\frac{d_2}{l_1},\ \frac{l_2-a_3}{l_2}=\frac{a_6}{l_3}=\frac{a_5+d_1}{l_4}$ $\frac{a_2+a_4}{l_3}=\frac{l_4-d_1-a_1}{l_4}$
29	$\frac{a_3}{l_2}=\frac{a_4}{l_3},\ \frac{d_1+a_1}{l_4}=\frac{l_1-d_2}{l_1}=\frac{d_3}{l_3},\ d_3=l_3-a_4$
30	$\frac{a_1+a_4}{l_1}=\frac{l_2-a_2}{l_2}=\frac{a_6}{l_3}=\frac{a_7}{l_4},\ \frac{a_3}{l_3}=\frac{a_5}{l_2}=\frac{a_4-d_1}{l_1}=\frac{d_2}{l_4}$
31	none
32	$\frac{a_1}{l_4}=\frac{a_2-a_5}{l_1}=\frac{a_6}{l_2}=\frac{a_7}{l_3},\ \frac{l_1-a_2-a_4}{l_1}=\frac{a_3}{l_2}$

References

[1] S. Foucault, C.M. Gosselin, Synthesis, design, and prototyping of a planar three degree-of-freedom reactionless parallel mechanism, Mech. Des. 126 (2004) 992–999.
[2] S. Briot, V.H. Arakelian, S. Guégan, PAMINSA: A new family of partially decoupled parallel manipulators, Mech. Mach. Theory 44 (2009) 425–444.
[3] V. Van der Wijk, S. Krut, F. Pierrot, J.L. Herder, Design and experimental evaluation of a dynamically balanced redundant planar 4-RRR parallel manipulator, Int. J. Robot. Res. 32 (6) (2013) 744–759.
[4] T. Laliberté, C. Gosselin, Synthesis, optimization and experimental validation of reactionless two-DOF parallel mechanisms using counter-mechanisms, Meccanica 51 (2016) 3211–3225.
[5] J. Karidis, G. McVicker, J. Pawletko, L. Zai, M. Goldowsky, R. Brown, R. Comulada, The hummingbird minipositioner – providing three-axis motion at 50 g's with low reactions, Proceedings of the IEEE International Conference on Robotics and Automation (1992) 685–692.
[6] G.W. Brown, Suspension system for supporting and conveying equipment, such as a camera, Patent US-4710819, 1987,
[7] B. Demeulenaere, P. Spaepen, S. Masselis, P. Cornelissen, G. Pinte, J. Hemelsoen, R. Boonen, K. Roelstraete, W. Desmet, J. Swevers, J. De Schutter, Experimental validation of input torque balancing applied to weaving machinery, Mech. Des. 130 (2) (2008) 022307.
[8] K. Ishida, T. Matsuda, Performance characteristics and working comfortableness of forest workers of a new non-vibrating chain saw utilizing perfectly balanced rotation-reciprocation device, in: Proceedings of the Fifth World Congress of Theory of Machines and Mechanisms, ASME, 1979, pp. 951–954.
[9] W.-K. Chung, H.S. Cho, On the dynamic characteristics of a balanced PUMA-760 robot, Ind. Electron. 35 (2) (1988) 222–230.
[10] M. Jean, C.M. Gosselin, Static balancing of planar parallel manipulators, in: Proceedings of the International of Conference on Robotics and Automation, 1996, pp. 3732–3737.
[11] T.G. Lim, H.S. Cho, W.K. Chung, Payload capacity of balanced robotic manipulators, Robotica 8 (1990) 117–123.
[12] T.G. Lim, H.S. Cho, W.K. Chung, A parameter identification method for robot dynamic models using a balancing mechanism, Robotica 7 (1989) 327–337.
[13] V. Van der Wijk, Methodology for analysis and synthesis of inherently force and moment-balanced mechanisms - theory and applications (dissertation), University of Twente. doi:10.3990/1.9789036536301, 2014.
[14] A. Martini, M. Troncossi, A. Rivola, Algorithm for the static balancing of serial and parallel mechanisms combining counterweights and springs: generation, assessment and ranking of effective design variants, Mech. Mach. Theory 137 (2019) 336–354.
[15] V.G. Arakelian, M.R. Smith, Shaking force and shaking moment balancing of mechanisms: a historical review with new examples, Mech. Des. 127 (2005a) 334–339.
[16] V.H. Arakelian, M.R. Smith, Erratum: shaking force and shaking moment balancing of mechanisms: a historical review with new examples, Mech. Des. 127 (2005b) 1035.
[17] V. Van der Wijk, J.L. Herder, B. Demeulenaere, Comparison of various dynamic balancing principles regarding additional mass and additional inertia, Mech. Robot. 1 (4) (2009) 041006.
[18] V. Van der Wijk, J.L. Herder, Dynamic balancing of mechanisms by using an actively driven counter-rotary counter-mass for low mass and low inertia, in: Proceedings of the Second International Workshop on Fundamental Issues and Future Research Directions for Parallel Mechanisms and Manipulators, Montpellier, 2008, pp. 241–251.
[19] R. Ricard, C.M. Gosselin, On the development of reactionless parallel manipulators, in: Proceedings of the ASME-DETC, 2000.
[20] Y. Wu, C.M. Gosselin, Design of reactionless 3-DOF and 6-DOF parallel manipulators using parallelepiped mechanisms, IEEE Trans. Robot. 21 (5) (2005) 821–833.
[21] J.F. Collard, C. Gosselin, Optimal synthesis of a planar reactionless three-degree-of-freedom parallel mechanism, Mech. Robot. 3 (041009) (2011) 1–9.

[22] S. Briot, I.A. Bonev, C.M. Gosselin, V. Arakelian, Complete shaking force and shaking moment balancing of planar parallel manipulators with prismatic pairs, Multi-body Dyn. 223 (K) (2009) 43–52.
[23] A. Martini, M. Troncossi, A. Rivola, Elastodynamic effects of mass-balancing: experimental investigation of a four-bar linkage, Adv. Mech. Eng. 5 (2013) 1–10.
[24] O. Fischer, Theoretische Grundlagen für Eine Mechanik der Lebenden Körper, Teubner, Leipzig, 1906.
[25] V. Van der Wijk, J.L. Herder, Synthesis method for linkages with center of mass at invariant link point - pantograph based mechanisms, Mech. Mach. Theory 48 (2012) 15–28.
[26] V. Van der Wijk, Design and analysis of closed-chain principal vector linkages for dynamic balance with a new method for mass equivalent modeling., Mech. Mach. Theory 107 (2017) 283–304.
[27] V. Van der Wijk, J.L. Herder, Inherently balanced 4R four-bar based linkages, in: Proceedings of the Robot Kinematics International Symposium on Latest Advances in Advances in Robot Kinematics, 2012, pp. 309–316. Lenarčič, J. and Husty, M. (eds.)
[28] V. Van der Wijk, On the Grand 4R Four-bar Based Inherently Balanced Linkage Architecture, in: Proceedings of the New Trends Mechanism and Machine Science 2016, MMS 43, 2017, pp. 473–480. P. Wenger and P. Flores (eds.)
[29] R. Kreutzinger, Über die Bewegung des Schwerpunktes beim Kurbelgetriebe, Getriebetechnik 10 (9) (1942) 397–398.
[30] V.A. Shchepetil'nikov, The determination of the mass centers of mechanisms in connection with the problem of mechanism balancing, Mechanisms 3 (1968) 367–389.
[31] V. Van der Wijk, J.L. Herder, The work of Otto Fischer and the historical development of his method of principle vectors for mechanism and machine science, in: Proceedings of the Fourth International Symposium on the History of Machines and Mechanisms, 2012, pp. 521–534. T. Koetsier, M. Ceccarelli (Eds.): Explorations in the History of Machines and Mechanisms
[32] L. Burmester, Die brennpunktmechanismen, Zeitschrift für Mathematik und Physik 38 (1893) 223 and 3.
[33] V. Van der Wijk, Mass equivalent pantographs for synthesis of balanced focal mechanisms, in: Proceedings of the Advances in Robot Kinematics 2016, 4, Springer Int. Publishing., 2018, pp. 1–10. Lenarčič, J. and Merlet, J.-P. (eds.)
[34] V.V. Dobrovol'skii, On the motion of the center of mass of a four-bar linkage, Mechanisms 3 (1968) 233–234.
[35] I.I. Artobolevskii, Theory of Mechanisms and Machines, Chap. XXV, Gos. Izdat. Tekh. -Teoret. Lit., Moscow, 1951.
[36] V. Van der Wijk, Spatial orientations of principal vector planes for inherent dynamic balancing., in: Proceedings of the Advances in Robot Kinematics 2018, Advanced Robotics, 8, Springer, 2019, pp. 302–309. In: Lenarčič, J. and Parenti-Castelli V. (eds)
[37] G.T. Bennett, A new mechanism, Engineering 76 (1903) 777–778.
[38] V. Van der Wijk, Shaking-moment balancing of mechanisms with principal vectors and momentum, J. Front. Mech. Eng. 8 (1) (2013) 10–16.